

DEPARTMENT OF THE AIR FORCE
HEADQUARTES, 603D REGIONAL SUPPORT GROUP (USAFE)
European Office of Aerospace Research and Development (EOARD)

Contract No. SPC 00-4032, F61775-00-WE032

awarded 24 March 2000

Final Report

Summarizing all progress on the tasks outlined in the proposal

Contract title: **Testing of the supersonic COIL driven by a jet SOG using a diode probe diagnostics and investigation of chemical generation of atomic iodine for COIL**

Investigators: **Otomar Špalek, Jarmila Kodymová
Vít Jirásek, Miroslav Čenský, Jan Kuželka**

Contractor: **Jarmila Kodymová
Department of Gas Lasers
Institute of Physics
Academy of Sciences of the Czech Republic
Na Slovance 2
182 21 Prague 8
Czech Republic
Phone : 420-2-66052699
Fax: 420-2-86890527
E-mail: kodym@fzu.cz**

Contractor signature:

Date: **4 April , 2001**

REPORT DOCUMENTATION PAGE

Form Approved OMB No. 0704-0188

Public reporting burden for this collection of information is estimated to average 1 hour per response, including the time for reviewing instructions, searching existing data sources, gathering and maintaining the data needed, and completing and reviewing the collection of information. Send comments regarding this burden estimate or any other aspect of this collection of information, including suggestions for reducing this burden to Washington Headquarters Services, Directorate for Information Operations and Reports, 1215 Jefferson Davis Highway, Suite 1204, Arlington, VA 22202-4302, and to the Office of Management and Budget, Paperwork Reduction Project (0704-0188), Washington, DC 20503.

1. AGENCY USE ONLY (Leave blank)		2. REPORT DATE 4 April 2001	3. REPORT TYPE AND DATES COVERED Final Report	
4. TITLE AND SUBTITLE Testing Of The Supersonic COIL Driven By A Jet SOG Using A Diode Probe Diagnostic, And Investigation Of The Chemical Generation Of Atomic Iodine For COIL			5. FUNDING NUMBERS F61775-00-WE	
6. AUTHOR(S) Dr. Jarmila Kodymova				
7. PERFORMING ORGANIZATION NAME(S) AND ADDRESS(ES) Institute of Physics Academy of Sciences Na Slovance 2 Prague 8 182 21 Czech Republic			8. PERFORMING ORGANIZATION REPORT NUMBER N/A	
9. SPONSORING/MONITORING AGENCY NAME(S) AND ADDRESS(ES) EOARD PSC 802 BOX 14 FPO 09499-0200			10. SPONSORING/MONITORING AGENCY REPORT NUMBER SPC 00-4032	
11. SUPPLEMENTARY NOTES				
12a. DISTRIBUTION/AVAILABILITY STATEMENT Approved for public release; distribution is unlimited.			12b. DISTRIBUTION CODE A	
13. ABSTRACT (Maximum 200 words) This report results from a contract tasking Institute of Physics Academy of Sciences as follows: The contractor will investigate the previously developed supersonic COIL driven by a jet singlet oxygen generator. Its operation will be explored using the tunable diode laser provided by AFRL. They will also investigate the chemical generation of atomic iodine for a COIL using apparatus designed and built under their previous contract(s).				
14. SUBJECT TERMS EOARD, Chemical oxygen iodine lasers			15. NUMBER OF PAGES 28	16. PRICE CODE N/A
17. SECURITY CLASSIFICATION OF REPORT UNCLASSIFIED	18. SECURITY CLASSIFICATION OF THIS PAGE UNCLASSIFIED	19. SECURITY CLASSIFICATION OF ABSTRACT UNCLASSIFIED	20. LIMITATION OF ABSTRACT UL	

NSN 7540-01-280-5500

Standard Form 298 (Rev. 2-89)
Prescribed by ANSI Std. Z39-18
298-102

STATEMENT

- (1) The Contractor, Institute of Physics of the Academy of Sciences, hereby declares that, to the best of its knowledge and believe, the technical data delivered herewith under Contract No. F61775-00-WE032 is complete, accurate, and complies with all requirements of the contract.**

- (2) I certify that there were no subject inventions to declare as defined in FAR 52.227-13, during the performance of the Contract No. F61775-00-WE032.**

Date: 3 April, 2001

Name and Title of Authorized Official:

Dr. Vladimír Dvořák
Director of Institute of Physics

Content

The tasks outlined in the proposal

1. Testing the COIL operation with constructionally modified jet singlet oxygen generator

- 1.1. Constructional modifications of the jet SOG
- 1.2. Additional improvements of the COIL device
- 1.3. COIL operation with the modified jet SOG

2. Testing the COIL by using the Iodine Scan diode probe laser diagnostics

3. Chemical generation of atomic iodine for COIL

- 3.1. Mathematical modeling of atomic iodine generation
 - 3.1.1. Description of modeling conditions
 - 3.1.2. Results and discussion
- 3.2. Experimental investigation of atomic iodine
 - 3.2.1. Experimental
 - 3.2.1.1. Experimental device
 - 3.2.1.2. Detection of generated atomic iodine
 - 3.2.1.3. Generation of chlorine dioxide
 - 3.2.1.4. Measurements of NO and HI flowrate
 - 3.2.2. Results and discussion
 - 3.2.3. Conclusions from experimental investigation

Appendix I

Appendix II

4. References

5. Acknowledgement

6. Project cost

The tasks outlined in the proposal

1. Testing the COIL operation with constructionally modified jet singlet oxygen generator (jet SOG)

The jet SOG with the vertical gas exit instead of the side exit was planned to be designed, constructed and employed. The aim of this modification was to solve a serious problem accompanying the jet SOG operation, i.e., a liquid (BHP) droplets escape with the gas exiting the generator. These droplets are partly evaporated and form a solid layer on the walls of the gas channel and nozzle throat, and partly fly as an aerosol into the laser cavity. This consequently diminishes a cross section of the channel and nozzle throat for the gas flow, causes a blocking the holes of small diameter in the iodine injector that is placed in the walls of gas channel, and can cause the light scattering on the aerosol particles in the gain region. As a whole, these effects result in a relatively low chemical efficiency of our COIL device so far.

2. Testing the COIL by using the Iodine Scan diode probe laser diagnostics

A frequency-stabilized, line-narrowed, single mode diode laser system was planned to be used as a small signal probe to determine a spatial gain and temperature distribution across the gain region of COIL device. The aim of this gain investigation was to compare the results with similar performed investigations on different laser systems in the AFRL and other European COIL Laboratories. It was originally planned that the diagnostics loaned from the US AFRL/DE for the use in the European COIL Labs has to be transferred to our laboratory from the Samara COIL Lab during August 2000.

3. Chemical generation of atomic iodine for COIL

A new method of chemical generation of atomic iodine applied in the COIL operation was planned to be proposed and investigated. The aim of this work was first the mathematical modeling of reaction systems for this process through either atomic fluorine or atomic chlorine, and on the basis of the modeling results to choose a more suitable reaction system for the experimental investigation. Further, the results of modeling should have to be utilized for a design of the experimental apparatus used for testing this reaction system and finding the experimental conditions for efficient production of atomic iodine for COIL. The Iodine Scan diode probe laser diagnostic for a direct detection of atomic iodine in the gas flow was planned to be used for the detection of I atoms generated by this method.

Ad 1. Testing the COIL operation with constructionally modified jet singlet oxygen generator

1.1. Constructional modifications of the jet SOG

The constructional modifications of the jet SOG were mostly aimed at suppressing an escape of the BHP (Basic Hydrogen Peroxide) droplets from the generator into the gas channel leading into the laser cavity. This unfavourable effect in the jet SOG operation is most probably the reason for the low chemical efficiency of this laser device.

A principal design of the jet SOG with a vertical gas exit instead of the jet SOG with a side (horizontal) gas exit employed previously was described in the interim Report 0001 of this contract. It is shown here only schematically in **Fig. 1**. A gas generated in the g/l reactor (2) of the generator exits through metal tubes (3) (either 8 tubes of \varnothing 8/6 mm or 4 tubes \varnothing 10/8 mm) fixed between the BHP injector plate (4) and the plate (5) dividing the cavity for BHP liquid loading and the upper gas cavity (6). By enlarging a cross-section of the gas stream crossing the last rows of liquid jets, and a sudden change of the gas flow direction in the gas cavity (6), we expected a substantial decrease in liquid droplets entraining with gas flowing into the laser cavity. A gas space of the upper part of this modified generator was reduced by two fillers to diminish a loss of singlet oxygen. Further, additional constructional changes were introduced recently also into the jet SOG with horizontal gas exit, as the very first results with the “vertical” generator did not bring an expected improvement of the laser operation and increasing in the chemical efficiency of this COIL device. The main modifications of both versions of the jet SOG and operation improvements are described bellow.

a) An effect of installation of BHP “directors” in the space above BHP injector in the jet SOG with horizontal gas exit

The idea of using the vane plates for flow stabilization of BHP jets was suggested and tested in the Korean COIL lab [1]. In the jet SOG used in our laboratory, the BHP directors were installed into the space above the BHP injector in the form of bunch of vertical tubes (welded together) of diameter 12/10 mm and length 50 mm (see the cross section in **Fig. 2**). It was

expected that they decrease a turbulence of BHP in this space, stabilize substantially BHP jets and so suppress a jets disintegration into droplets. Several experiments with this modified generator did not prove a better jet SOG operation with less BHP droplets escape and increase in the laser power.

b) An effect of higher BHP jets velocity

In the first laser experiments employing the jet SOG with vertical gas exit, the BHP jets velocity was 5.7 m/s. It was desirable to increase the jets velocity (above all at higher gas velocities) to suppress BHP droplets escaping. It could be achieved by a substantial increase in a pressure drop across the BHP injector (6 mm-thick plastic plate with 0.8-mm holes), which could bring however some problems with BHP pumping. In using of thinner plate for the injector fabrication, a non parallel streaming of jets could occur, and there would be also a danger of its breaking. We therefore improved the previous injector by enlarging the diameter of holes in the upper part of the plate up to 1.2 mm (into 3 mm-depth), while the diameter of holes in the bottom part remained 0.8 mm. This modification made possible to increase the jets velocity up to 8.2 m/s at the same pressure drop across the plate. A testing the COIL operation driven with this jet SOG showed that the droplets escaping from the generator was suppressed to some extent and the output power was higher.

c) An effect of geometry of the gas exit from the generator

An effect of arrangement and diameter of cylindrical channels through which the gas containing singlet oxygen exits the generator (see **Fig. 1**) was investigated. Two arrangements of the metal tubes forming these channels were tested: 8 tubes of 6 mm i.d. arranged in two rows, and 4 tubes of 8 mm i.d in one row. Testing both arrangements during the generator and laser operation did not prove any different effect.

d) An effect of introducing a part of primary helium downstream the reactor

An effect of lowering a flowrate of the primary helium, He_{prim} , admixed into chlorine on the liquid droplets escape was investigated. For this purpose, He_{prim} was divided into two flows -

the first one was admixed into chlorine injected in generator and the second one was introduced into the gas flow exiting the reactor. Two arrangements were tested:

1/ a part of He_{prim} was introduced into the gas space (6 in Fig.1) upstream the throttle valve.

2/ a part of He_{prim} was injected into the gas channel downstream the throttle valve.

In the first case, helium introduced into the upper gas space in the generator increased the pressure in the g/l reactor resulting in a lowering the singlet oxygen yield. This arrangement required therefore a simultaneous control of the throttle valve position. In the second case, helium was injected from the tube of 8/6 mm in diameter with two rows of holes (0.8 mm i.d.) oriented 45° to the axis of the gas channel. The experimental testing of both modifications showed that the second arrangement was more advantageous and led to some (but not sufficient) suppression of liquid droplets escape.

e) An effect of needles around the gas outlet tubes in BHP injector

In the first version of the jet SOG with vertical gas exit, one row of needles (1.2/0.9 mm in diameter and 30-45 mm long) was installed around the gas outlet tubes in BHP injector (similarly as in the jet SOG with horizontal gas outlet). The needles were removed later and it was proved that it suppressed substantially the liquid escaping and increased simultaneously the laser output power. This was ascribed to an unfavourable effect of liquid layer formed by spread jets and flowing down along the needles, which can be then captured into the exiting gas.

f) An outgassing of BHP solution before starting the generator operation

A BHP outgassing before starting with the generator operation is quite necessary to suppress a disintegration of jets. It is caused by bubbles of oxygen formed due to both peroxide decomposition and chlorinating reaction during the previous experimental run. The outgassing proceeds very effectively during the BHP jetting and at a simultaneous evacuation of the BHP tank. In this way, the BHP outgassing is finished within less than one minute.

g) An effect of dissolved oxygen and gas bubbles on the generator operation

This phenomenon is the most serious and not satisfactorily solved problem up to now in continuous operation of the jet SOG. Oxygen arising mainly from the reaction of chlorine with

BHP is present partly in the form of oversaturated solution and partly as gas bubbles. Bubbles circulate with the BHP solution from the tank to the upper part of the jet SOG, and on passing the liquid through the BHP injector, a considerable drop in pressure occurs (e.g. from 200 kPa to 10 kPa). It causes a substantial drop in oxygen solubility in BHP solution (20 times for the given example) and so most of dissolved oxygen is transferred into the gas phase. A volume of each bubble is considerably enlarged (20 times, for the given example) resulting in a partial disintegration of jets into droplets that can be easily captured by gas exiting the generator. Even though the BHP solution is outgassed at the beginning of the operation, it is saturated very fast by oxygen. For example, 15 litres of the outgassed BHP solution circulating between the tank and generator with the rate of 100 l/min is supplemented by the solution saturated with oxygen (in both forms) within 9 s only. As a result, the amount of liquid droplets captured into the exiting gas increases with the generator running time, and consequently water vapour pressure, as well as the light scattering on droplets in the laser gain region, become a serious problem. Both effects cause a decreasing the laser output power. This is unfavourable and still unresolved feature of jet generators. On the other hand, the effect of the BHP temperature increase during the SOG operation which also results in a higher water vapour pressure is well managed in jet type of singlet oxygen generators.

h) An optimization of automatic control of jet SOG and COIL operation

Many experiments were performed with a different chronology of individual controlling operations in order to avoid above all a pressure shock in the generator due to some inconvenient sequence of operations (opening gas valves, the gate valve, the laser by-pass valve, etc.), or improper adjustment of the throttle valve, which could result in an undesirable liquid capture into the gas channel. An example of the optimized procedure during the COIL operation is presented in the **Appendix I**.

1.2. Additional improvements of the COIL device

a) Several improvements of the iodine management were made resulting in a more reliable control of He_{sec} flow through the I_2 tank and by-passing this tank, and so a better control of the

iodine flow rate into the laser. Helium flowing through both lines is measured independently and recorded on-line.

b) A system of automatic control of the COIL operation with the special hardware and software was originally designed and developed. This controlling system pursues the following operations:

- controlling the operation of the BHP pump (including BHP flowrate),
- opening and shutting the valves for primary gases (i.e. Cl_2 , He_{prim} admixed into Cl_2 , He_{prim} injected into the main gas flow downstream the generator),
- opening and shutting the valve between the I_2 tank and I_2 injector,
- opening and shutting the flat gate valve, the valves closing the laser by-pass tube, and the tube by-passing the I_2 injector,
- adjusting an opening of the throttle valve, and so adjusting the generator pressure,
- adjusting an opening of two proportional valves controlling a) He_{sec} flowrate through the I_2 tank, and b) He_{sec} flowrate through the tube by-passing the tank; in this way, to maintain a required overall He_{sec} flowrate (and the penetration factor),
- evaluating a signal from the spectral photometer used for measuring the I_2 concentration; by means of this value, a measured pressure and temperature in the optical cell for I_2 detection, and He_{sec} flowrate, evaluation of the actual I_2 flowrate in the laser and adjusting a position of the proportional valves for two flows of He_{sec} .

c) Parameters automatically controlled (every 0.5 s):

- total flow rate of He_{sec} ,
- I_2 flowrate

b) Parameters recorded and evaluated on-line

- pressure in the BHP tank, generator, optical cells for $\text{O}_2(^1\Delta_g)$, $\text{O}_2(^1\Sigma)$, Cl_2 , and I_2 detection, and laser cavity,
- BHP temperature in BHP tank and generator,
- gas temperature in optical cells for $\text{O}_2(^1\Delta_g)$, $\text{O}_2(^1\Sigma)$, Cl_2 , and I_2 detection, and laser cavity,
- partial pressure of $\text{O}_2(^1\Delta_g)$,
- partial pressure of $\text{O}_2(^1\Sigma)$,
- I_2 concentration and I_2 flowrate,

- flowrates of all gases,
- temperature of I₂ management (I₂ tank, I₂ cell, I₂ delivery tubes, I₂ injector),
- laser output power.

c) Parameters evaluated off-line

- O₂(¹Δ_g) yield,
- partial pressure of H₂O,
- dilution ratio for I₂, i.e. n_{He_{sec}}/n_{I₂},
- relative penetration factor, Π_r, i.e. a ratio of the penetration parameter, π, to the full penetration parameter, π_{full} (defined in the Report 0001),
- cross-section of unblocked holes of I₂ injector (overall cross-section compared with the cross-section evaluated from flow parameters under sonic conditions) – an actual cross-section of injector holes during measurements enables to recognize a blocking some holes by solid (precipitated) I₂ or BHP solid films (see the Report 0001).

1.3. COIL operation with the modified jet SOG

The constructed jet SOG provides relatively high O₂(¹Δ_g) yields even if the generator pressure is relatively high. The data for 40 mmol Cl₂/s and 80 mmol He_{prim}/s are given in **Table 1**.

Tab. 1

P_G, kPa	3	5	8	10	12	15
(Torr)	(22.5)	(37.5)	(60)	(75)	(90)	(112.5)
Y_Δ, %	80	74	65	58	52	43

An example of the more important experimental data recorded and evaluated automatically during each experimental run is presented in **Figs. 3 - 6**. **Fig. 3a** shows the recorded time course of flowrates of chlorine, primary helium admixed into chlorine, primary helium injected downstream the generator, secondary helium flowing through the I₂ tank, secondary helium bypassing the tank it, and overall secondary helium. In **Fig. 3b**, the time course of the generator

pressure, the pressure in $O_2(^1\Delta_g)$ optical cell, the $O_2(^1\Delta_g)$ partial pressure, and the pressure in laser cavity are plotted.

Figs. 4a and **4b** illustrate the time course of iodine concentration, BHP jets temperature and BHP temperature in tank, and temperature in the optical cell for $O_2(^1\Delta_g)$ detection. In **Figs 5a** and **5b**, the time course of the evaluated penetration factor, dilution ratio, iodine molar flow rate, and laser output power is plotted. **Fig. 6a** and **6b** show the time course of pressure and temperature in the iodine cell, and the evaluated cross-section area of unblocked openings in the I_2 injector (calculated as described in the Report 0001).

The recording and evaluation of all these parameters make possible to check the function of all important parts of the laser system. In the presented figures, e.g., the choking the gas flow exiting the generator (between 190 s and 200 s) resulted in an increase in the generator pressure, a lowering the $O_2(^1\Delta_g)$ partial pressure (including the 1.315 nm radiation), and also the laser output power. During this measurement no blocking of iodine injector openings by BHP particles was observed (see **Fig 6b**). As a result, no increase in pressure in the I_2 cell was observed (see **Fig. 6a**), as well as, no worsening of the laser output power. From **Fig. 5b** follows, that the optimum laser power was attained at 1.5 mmol I_2/s , lower value at 1.25 mmol I_2/s , and the least value at 1.75 mmol I_2/s . The relative penetration factor was lower than the optimum value, whereas the dilution ratio of iodine was in optimum region (see **Fig. 5a**). The time dependence of BHP temperature in tank, BHP jets temperature, and temperature in the optical cell showed a quite normal course.

These plots are presented to show that the controlling of all these parameters is on a relatively good level. There may be two reasons only due to which a higher laser output power (above 500 W at 40 mmol Cl_2/s) and better chemical efficiency of this COIL was not achieved: a) BHP droplets streaming into the laser gain region, and b) resonator mirrors quality. We suppose that the first reason causes the main current limitations of our COIL device. As some recent modifications of the jet SOG (e.g. removing the needles surrounding the gas exit – see above) helped to decrease the amount of BHP droplets escaping from the jet SOG, we hope that the next development in the COIL testing could be more successful.

Ad 2. Testing the COIL by using the Iodine Scan diode probe laser diagnostics

For the objective reason, a planned testing of the supersonic COIL by a diode probe diagnostics could not be performed during the contract duration. This diagnostics lent by the US AFRL/DE for the use in the European COIL Laboratories (DLR Lab, Samara COIL Lab, and Prague COIL Lab) was to our disposal not until the end of January 2001 (at the time of the proposal preparing for this contract, we supposed that the diagnostics will be in our lab since the August 2000). Dr. Gordon Hager, the contractor manager, from the AFRL/DE has been acquainted with this situation and suggested to use the diagnostic first for solving the task concerning the chemical generation of atomic iodine. We suppose that this diagnostics instrument will be used form the COIL gain investigation during the second half of this year if the new contract with the EOARD is concluded.

Ad 3. Chemical generation of atomic iodine for COIL

3.1. Mathematical modeling of atomic iodine generation

The one-dimensional modeling of chemical generation of atomic iodine through chemically produced atomic fluorine and atomic chlorine, respectively, was presented in the Report 0002 of this contract. This modeling was performed under conditions typical for the subsonic region (i.e. in the gas channel upstream of the nozzle) of the conventional 1kW-class supersonic COIL. It was aimed at the investigation of possibility to generate atomic iodine directly in this laser instead of its production by the dissociation of molecular iodine. The results of this modeling proved that the system via atomic chlorine is more advantageous for the laser conditions, and has been therefore chosen for the experimental verification on a small-scale experimental apparatus. The set up is described in detail in the Report 0001, and in the chap. 3.2 of this Report. In the next section, the modeling of I atoms production in conditions characteristic for this small scale device is presented. This modeling included, in comparison with the previous modeling, the extended set of kinetic equations with several additional chemical reactions.

3.1.1. Description of modeling conditions

Similarly as in the previous model, the following assumptions were considered: an instantaneous mixing of reactants, neglecting the heat transfer and adiabatic conditions. The calculations were performed for the following flowrates of reactants used typically in operation of the small-scale experimental apparatus:

Reactant	Flowrate, $\mu\text{mol/s}$
ClO_2 (prim.flow)	160-360
NO (1 st injector)	160-200
NO (2 nd injector)	160-200
HI (3 rd injector)	100-300
Residual Cl_2	10-25

All reactants were diluted by nitrogen, and a resulting total N_2 flow rate was 8-10 mmol/s (see chapter 3.2.). A total pressure of the gas mixture measured in the first optical cell for I_2 detection by the Ar ion laser (see **Fig. 10** and **Photo 1**) was typically 2-3 kPa. Temperature of the gas mixture measured in the same place varied from 330 to 350 K. The calculated volume flowrate of gas mixture was about 8 l/s which is higher than the value corresponding to the pumping capacity of the rotary pump (6.9 l/s). It can be ascribed to a suction effect of the liquid nitrogen trap employed.

The set of chemical reactions involved into the kinetic model and their rate constants (in $\text{cm}^3\text{molec}^{-1}\text{s}^{-1}$ for bimolecular reactions, and $\text{cm}^6\text{molec}^{-1}\text{s}^{-1}$ for trimolecular reactions) are listed in the **Table 2**. This set is extended, in comparison with the modeling presented in the Report 0002, by the reactions (7)-(12), (19), (23)-(25). The reaction between the residual molecular chlorine and hydrogen iodide (24) produces significant amount of molecular I_2 in the tube between the first and second detection place of I_2 where the gas flows relatively slowly (4m/s). The rate constant of this reaction was found experimentally in our laboratory (see Report 0002). Further, the reactions with the radical ClOO (9-11), and two reactions of ICl (22,23) were added, using their published rate constants. The rate constants for the reactions (7), (10), (12), (13), (17), and

(22) are valid for M = He as a buffer gas, but they were used also in our calculations due to inaccessible values for N₂ used in our experiments.

Tab. 2

Reaction		Rate constant, cm ³ molec ⁻¹ s ⁻¹ , or cm ⁶ molec ⁻¹ s ⁻¹	Reference
1.	ClO ₂ + NO → ClO + NO ₂	$k_1 = 3.4 \times 10^{-13}$	[2]
2.	ClO + NO → Cl + NO ₂	$k_2 = 1.7 \times 10^{-11}$	[2]
3.	Cl + ClO ₂ → 2 ClO	$k_3 = 5.9 \times 10^{-11}$	[2]
4.	Cl + NO ₂ + He → NO ₂ Cl + He	$k_4 = 7.2 \times 10^{-31}$	[2]
5.	ClO + NO ₂ + He → NO ₃ Cl + He	$k_5 = 1.0 \times 10^{-31}$	[2]
6.	Cl + NO ₂ Cl → Cl ₂ + NO ₂	$k_6 = 3.0 \times 10^{-11}$	[2]
7.	Cl + NO + M → NOCl + M	$k_7 = 9.0 \times 10^{-32}$	[2]
8.	Cl + NOCl → Cl ₂ + NO	$k_8 = 3.3 \times 10^{-11}$	[2]
9.	ClO + ClO → Cl + ClOO	$k_9 = 2.8 \times 10^{-14}$	[2]
10.	ClOO + M ↔ Cl + O ₂ + M	$k_{10} = 1.3 \times 10^{-14}$ $k_{-10} = 5.6 \times 10^{-34}$	[2] [2]
11.	Cl + ClOO → 2 ClO	$k_{11} = 1.0 \times 10^{11}$	[2]
12.	ClO + ClO + M → Cl ₂ + O ₂ + M	$k_{12} = 6.6 \times 10^{-32}$	[2]
13.	Cl + Cl + M → Cl ₂ + M	$k_{13} = 6.4 \times 10^{-33}$	[2]
14.	HI + Cl → I + HCl	$k_{14} = 9.6 \times 10^{-11}$	[3]
15.	I + I + N ₂ → I ₂ + N ₂	$k_{15} = 4.2 \times 10^{-32}$	[4]
16.	I + I + I ₂ → 2 I ₂	$k_{16} = 3.7 \times 10^{-30}$	[5]
17.	I + NO + M → INO + M	$k_{17} = 1.38 \times 10^{-32}$	[6]
18.	INO + I → I ₂ + NO	$k_{18} = 2.63 \times 10^{-10}$	[6]
19.	I + NOCl → ICl + NO	$k_{19} = 6.2 \times 10^{-12}$	[2]
20.	I + NO ₂ + N ₂ → INO ₂ + N ₂	$k_{20} = 3.1 \times 10^{-31}$	[6]
21.	I + INO ₂ → I ₂ + NO ₂	$k_{21} = 8.3 \times 10^{-11}$	[6]
22.	I + Cl + M → ICl + M	$k_{22} = 1.0 \times 10^{-32}$	[2]
23.	Cl + ICl → Cl ₂ + I	$k_{23} = 8.0 \times 10^{-12}$	[2]
24.	2 HI + Cl ₂ → I ₂ + 2 HCl	$k_{24} = 1.94 \times 10^{-16}$	[this work]
25.	HI + NO → HNO + I	$k_{25} = 1.47 \times 10^{-16}$	[7]

In the model for chemical generation of atomic iodine by the suggested method directly in the supersonic COIL under conditions of subsonic or transonic mixing of given reactants with the primary gas flow containing mainly O₂(¹Δ_g), one should take into consideration also reactions of the reactants, intermediates, and products of this reaction system with the components of the

COIL medium, mainly with singlet oxygen, $O_2(^1\Delta_g)$, and the excited atomic iodine, $I(^2P_{1/2})$. The quenching constants of these species for some compounds are listed in **Table 3**.

Tab. 3

Quenching of $O_2(^1\Delta_g)$ and $I(^2P_{1/2})$ by components present in the reaction system for I atoms generation

		$k, \text{cm}^3 \text{molec}^{-1} \text{s}^{-1}$	Reference
$O_2(^1\Delta_g)$	$O_2(^1\Delta_g)$	1.7×10^{-17} (1)	[8]
	$O_2(^1\Delta_g)$	2.7×10^{-17} (2)	[8]
	ClO_2	5×10^{-17}	[9]
	HI	2×10^{-17}	[10]
	HCl	4×10^{-18}	[10]
	NO	5×10^{-17}	[10]
$I(^2P_{1/2})$	NO_2	5×10^{-18}	[11]
	HI	5×10^{-14}	[12]
	HCl	6.5×10^{-15}	[12]
	H_2O	2.3×10^{-12}	[13]
	I_2	3.5×10^{-11}	[8]
	Cl_2	8.0×10^{-15}	[8]
	$O_2(^1\Delta_g)$	1.1×10^{-13}	[8]

(1) – self-quenching reaction, (2) – pooling reaction

The data for ClO_2 , NO, NO_2 , HCl, and HI show that these molecules quench $O_2(^1\Delta_g)$ only weakly. The quenching constants are comparable with the rate constants of $O_2(^1\Delta_g)$ self-quenching and pooling reactions (see also Tab. 3). Since concentration of these compounds in the reaction system is much lower than the concentration of $O_2(^1\Delta_g)$ in the COIL medium, their quenching effect may be neglected. A quenching of the excited iodine atoms, $I(^2P_{1/2})$, by HCl and HI molecules may be also neglected. The data on quenching of $I(^2P_{1/2})$ atoms by other species of the reaction system (ClO_2 , NO, and NO_2) has not been found in the literature.

The effect of exhausting the reactants, ClO_2 , NO, and HI in the reaction with $O_2(^1\Delta_g)$ during atomic iodine generation was estimated from the fact that reaction rates of these processes cannot exceed the quenching rate of $O_2(^1\Delta_g)$ by these compounds. On the basis of this

consideration, the reactants exhausting by $O_2(^1\Delta_g)$ may be neglected in comparison with the reaction rates included in the generation of I atoms.

3.1.2. Results and discussion

Atomic iodine production in a small-scale device

Figs. 7-9 show a time course of the flowrates of reactants and products in the reaction system from the moment of the first injection of NO. The plots are calculated for the molar flowrate ratio of $ClO_2 : NO(I+II)$ equal to 1:2, 1:1.5, and 1:1, respectively (NO(I+II) means a sum of NO flowrate through the first and second injector). In agreement with the previous modeling for the conditions in COIL, the highest yield of atomic iodine is obtained for the ratio of $ClO_2 : NO(I+II) = 1 : 2$. A maximum value of I flowrate of $90 \mu\text{mol/s}$ that was achieved $70 \mu\text{s}$ after HI injection corresponds to 56 % of the initial ClO_2 flowrate. For the $ClO_2 : NO(I+II)$ ratio equal to 1:1.5, and 1:1, a maximum I flowrate of $55 \mu\text{mol/s}$ and $20 \mu\text{mol/s}$, respectively, is achieved. The calculated values of I_2 flowrate in the location of both optical cells for I_2 detection are shown in bottom parts of these figures. A remarkable increase in the I_2 flowrate detected in the second cell is caused by an additional formation of molecular iodine by the slow reaction (24) in a large volume of the tube between the both cells. An increase in the initial flowrate of HI over the equimolar ratio causes an increase in I_2 flowrate detected in the second cell, but does not affect it in the first cell. This result proves that all I_2 molecules detected in the first cell should come only from the recombination of produced atomic iodine. This was confirmed also by calculations in which the reaction (24) was not included, providing the same I_2 flowrate in both detection cells for all investigated flowrate ratios of reactants. In **Figs. 7-9**, there are designated also locations of formerly and presently used constructional versions of the optical cells for the direct detection of I atoms by the diode probe laser diagnostics. It can be seen in **Figs. 7 and 8** that no I atoms should be detected in the formerly used optical cell as they are recombined to I_2 molecules before reaching this cell. If the flowrate of ClO_2 is higher (**Fig.9**), the reaction zone for I atoms production is rather extended, and a slight signal of I atoms could be also detected in this cell. In the presently used cell (characteristic by much shorter path between the place of production and detection of I atoms), the calculated average value of I atoms flowrate corresponds to 6.7 % of

the maximum value, and 5.4 % of the total iodine flowrate (calculated from the I₂ flowrate measured in the first optical cell). However, in case of the flowrate ratio of ClO₂ : NO = 1:1, atomic iodine is formed on the longer reaction path, and thus up to 75 % of the maximum flow rate, and 30 % of the total flow rate can be detected by the diode probe laser diagnostics. It must be considered, however, that a limited mass transfer rate of reactants (which was not included into the model) can prolong substantially the concentration profiles.

Further findings from modeling

The results of calculations showed that the reaction (25) can produce significant amount of atomic iodine only in the case of large excess of HI and NO. This was deduced from the finding that the amount of HNO produced in this reaction was negligible at usual flowrates of HI and NO.

It follows from **Fig. 9**, that the high amount of ClO is formed at the high ClO₂ : NO ratio downstream the NO(II) injection, and reacts subsequently with NO₂ by the reaction (5). In this case, 40% only of the formed NO₂ flows through the first cell for I₂ detection.

The calculations of adiabatic reaction temperature predict the rapid temperature rise, firstly caused by the reaction (2) (by about 60 K), and then by the reaction (14) (by further 40 K).

3.2. Experimental investigation of atomic iodine

3.2.1. Experimental

3.2.1.1. Experimental device

A design and construction of a small-scale device for the experimental investigation of chemical generation of atomic iodine (including calculations for designing the injectors of reactants) was described in detail in the interim Reports 0001 and 0002 of this contract.

3.2.1.2. Detection of generated atomic iodine

In the first experimental arrangement, the reaction gas mixture flew from the reactor into the first optical cell (gas transfer time of 5 ms) and followed into the second detection cell (gas

transfer time of 88 ms). The second cell located in a relatively long distance was originally designed for the case of remarkable mass transfer limitation of the reactions that could stretch substantially the reaction zone. In these cells oriented perpendicularly to the gas flow, the concentration of molecular iodine was measured by the absorption photometry at 488 nm using the Argon ion laser. Molecular iodine measured in the first cell is produced, according to the modeling (see chap. 3.1.2), by the recombination of generated iodine atoms only. Consequently, the production rate of atomic iodine can be calculated from I_2 concentration in this cell and the gas volume flow rate. In the experiments described in the Report 0002, an effect of reactions of HI with residual Cl_2 (eq. 24) and NO (eq. 25) on the production rate of molecular iodine was studied. It was proved experimentally that a contribution of molecular iodine produced by these reactions is negligible in the first optical cell, but is significant in the second cell. During detection of atomic iodine, contributions of these reactions must be therefore subtracted from the measured I_2 flow rate through the second cell to evaluate properly the rate of I atoms generation (mainly at higher concentrations of residual Cl_2 and NO).

At the end of January 2001, the experimental apparatus was supplied with a direct detection of atomic iodine using the Iodine Scan diagnostics with a tunable diode probe laser. It was developed by the Physical Science Inc. and is described in detail in the instructional materials provided by the AFRL. It is based on sensitive absorption spectroscopy by means of tunable near infrared diode laser monitoring the gain or absorption for the $I(^2P_{1/2}) - (^2P_{3/2})$ transition at 1315 nm. The laser frequency is scanned over the I transition in a double pass configuration through the optical cell. The frequency is calibrated by the Fabry-Perot interferometer. The data of the monitored gain are processed by PC on-line with the special developed software. The scheme of the diode probe diagnostics beam is schematically shown in **Fig. 10**. This direct I atoms detection is employed now simultaneously with the indirect method of I atoms determination from I_2 flow rate. The new experimental arrangement is schematically shown in **Fig. 11 and Photos 1 and 2**. The gas exiting the reactor is introduced first into the optical cell for detection of atomic iodide (11) through which it flows longitudinally, and then it enters the first optical cell (12) and the second optical cell (13) for detection of molecular iodine.

The cell for I atoms detection (11) is 11 mm i.d. In the first experiments, it was 10 cm of inner length and connected through 5cm-long tube of 10 mm i.d. with a quick coupler to the

reactor. In order to shorten the path of atomic iodine flow from the reactor to the place of its detection, a shorter cell (45 mm) is used presently which was welded directly to the reactor wall. The axis of both tubes (reactor and cell) are skew lines forming an angle 90° . The planar glass windows formerly used were replaced by the glass wedge (3°) to reduce a signal noise of the diode probe laser. The gas path from the holes of the third injector (I#3) to the entrance of the cell (11) was 6 cm for the former cell, and 1.5 cm for the presently used cell. A transport time of gas from the holes of the injector I#3 to the entrance of the cell (11) was 0.6 ms for the former cell, and 0.15 ms for the presently used cell (1.8 ms and 0.7 ms, respectively, till the cell end). By the results of modeling, the concentration of I atoms detectable in the former optical cell is nearly zero. At the entrance to the new (presently used) optical cell is typically 20 % of the maximum attainable concentration, and 1 - 3 % only at the cell end (see chap. 3.1.2.). It means that the concentration of I atoms measured in the new detection cell represents only a fraction of the maximum attainable value. Considering a limited mass transfer rate of reactants, the reaction path however may be more extended and the concentration of atomic iodine in the optical cell (11) may be higher than the above values. For these reasons, even though the diode probe diagnostics is a direct method for atomic iodine detection, it cannot provide overall values of I atoms production. It would be possible only in the case of measuring a dependence of the local I atoms concentration on a distance from reactor and at perpendicular orientation of the optical cell to the gas flow direction. This could be realized only at higher flow rates of atomic iodine (planned for the application in COIL) making possible to enlarge the width of gas channel and so to measure with a perpendicular orientation of the optical cell to the gas flow. In the used experimental arrangement, the total rate of I atoms production can be properly estimated from the concentration of molecular iodine in the first optical cell for I_2 detection (12) where the recombination of I atoms is finished.

3.2.1.3. Generation of chlorine dioxide

Chlorine dioxide, ClO_2 , used as a reactant for atomic chlorine production was generated by the reaction



In the first experiments, the column generator filled with 3.6 dm³ of powdered NaClO₂ (80 % w/w) was used. Later, a bigger generator was employed containing 10 dm³ of the crystalline chlorite (50 % w/w). It reacted with gaseous chlorine diluted with buffer gas (nitrogen) (1:25) passing through the column at atmospheric pressure. The former generator produced 80 – 120 μmol ClO₂/s with ClO₂ yield of 75 %, the bigger generator then 140 – 160 μmol ClO₂/s with the yield of 83 %. It was however found during the experimental work that the reactors productivity decreased gradually with time, even if the degree of chlorite depleting was rather low. For example, about a half ClO₂ yield only was obtained at 12 – 15 % conversion of NaClO₂ to NaCl in comparison with the initial ClO₂ yield. It is probably caused by forming a sodium chloride layer on the surface of chlorite crystals which hinders the Cl₂ diffusion and slows the overall process.

In searching for a more effective and stable production of ClO₂, we tested also an industrially used ClO₂ production that is based on the reaction of gaseous Cl₂ with NaClO₂ solution. We have tested this method by bubbling Cl₂ diluted with N₂ (1:40) through 40 % solution of NaClO₂. In this way, a much smaller generator could be employed, e.g., 1 liter of NaClO₂ solution produced 200 – 250 μmol ClO₂/s with the yield of 81 – 85 % during 5 hours up to about 90 % depletion of chlorite. A disadvantage of this process consists in some content of water vapor in the generated gaseous ClO₂ but it can be reduced by lowering the solution temperature or using a water vapor trap. At a temperature of the chlorite solution of 0°C (or the trap temperature of – 5°C), the water vapor partial pressure in the gas mixture with 4 kPa of ClO₂ could be ~ 0.4 kPa which would increase the total content of water vapor by 0.4 – 0.8 % only after mixing with the primary gas stream containing singlet oxygen. It means that this contribution of water vapor is lower by one order than that coming from the singlet oxygen generator.

A flow rate of ClO₂ was determined from the chemical analysis based on bubbling the gas through 2 x 100 ml of 2.5 % solution of KI during 30 sec. The details of this analysis are presented in the Appendix I of the Report 0002.

3.2.1.4. Measurements of NO and HI flowrate

A flow rate of NO through each injector was determined from the declared composition of the NO + N₂ mixture (10 % w/w), and the flowrate of this mixture. This flowrate was determined from the pressure measured before the orifice through which the mixture flew with the sonic speed. In the same way, the flow rate of HI was calculated. A composition of the mixture of HI with N₂ was calculated from the analysis of the solution obtained by bubbling the gas mixture through 2 x 100 ml of distilled water. The argentometry was used for analysis of HI solutions (**Appendix II** of this Report). The alkalimetric analysis was used as a comparative method, which gave approximately the same results. The results of analyses (see **Appendix II**) proved that the composition of HI + N₂ mixture flowing from the gas cylinder is not stable and can vary with time due to a sedimentation of much heavier hydrogen iodide (M.W. 128 against 28 for nitrogen). It will be therefore more advantageous for using in the COIL system with higher flow rates of reactants to mix HI with the carrier gas just before its introduction into the HI injector. This procedure is not suitable for the described small-scale device as it would require to use a too small orifice in the measuring diaphragm (< 0.3 mm) which could be easily blocked by precipitated iodine or some corrosion products.

3.2.2. Results and discussion

Preliminary results of experimental investigation on atomic iodine generation were presented in the interim Reports 0001 and 0002 of this contract. The first experiments proved that atomic iodine can be generated effectively by the suggested method via chemically generated atomic chlorine. The chemical efficiency of I atoms generation exceeded in some measurements 50 % (related to the ClO₂ flowrate). In the next experiments described in the Report 0002, it was found that the rate of I atoms generation was increasing with increasing flow rate of HI. It was further found that the distance between the injector I#1 (the injection of the first part of NO) and the injector I#2 (the injection of the second part of NO) in the range of 8 – 21 mm did not affect the efficiency of I atoms production. It proved a substantial stability of ClO radical that was the main reaction product in this region (downstream the injector I#1) where the reaction of ClO₂ with NO

(in the equimolar ratio) occurs (eq. 1). The flow of atomic iodine in these measurements was detected by means of the absorption photometry at 488 nm only. The yield of atomic iodine calculated from I₂ concentration measured in the optical cell 12 ranged from 20 to 35 %. The calculations were based on the assumption that the content of HI in mixture with N₂ was 10.5 %, which resulted from pressures measured during the gas mixing. A subsequent analysis of HI + N₂ mixture proved a remarkable decreasing the HI content in gas discharged from the gas cylinder that was standing for several days (examples of this analysis are in **Appendix II**). It follows from this finding that the actual flow rates of HI were lower than values presented in the Report 0002 and, the actual values of the yield of atomic iodine were higher.

Since January 2001, atomic iodine flow rate was evaluated by means of the diode probe diagnostics simultaneously with its evaluation from the molecular iodine detection. **Figs. 12** and **13** show the examples of the time dependence of atomic iodine flow rate obtained by both techniques. It can be seen from the plots in **Figs. 12** and **13** that the I flows measured by both methods varied in a similar way. The measured flowrates of NO through the first and second injectors and HI through the third injector together with the gas temperature measured in the cell 12 are also shown in **Figs. 12** and **13**. In these measurements, the optical cell 11 for the direct detection of I atoms was of the first design (i.e. 10 cm long and connected with the reactor by a tube). In a qualitative agreement with the modeling results, the I flow rates evaluated from these measurements are lower in comparison with the values obtained from I₂ detection representing the overall production rate of atomic iodine. There is however a quantitative discrepancy between the theory and experiment. According to the modeling, a negligible proportion of generated atomic iodine could be detected in the used cell (see chap. 3.1.1.2). Much higher I flowrates measured by the diode probe diagnostics can be explained by a limited rate of the reactants mixing which stretches the zone of atomic iodine also into this optical cell.

From the measured flow rates of reactants, pressure and temperature, the relative penetration factors, i.e. the ratio of penetration parameter π to π_{full} (see the Report 0001) for all the secondary gases were evaluated after each experiment to obtain an information about the mixing conditions. A flow rate of produced nitrogen dioxide (NO₂) was also evaluated from an increase in the radiation absorption at 488 nm after admixing NO to the primary flow of ClO₂ by using the published absorption cross-section of $2.7 \times 10^{-19} \text{ cm}^2$ [14]. This value was used for a rough

estimation of the overall rate of reactions (1) and (2). A number of measurements was performed for different molar flow rates of reactants and different distances between injectors. It follows from these data that the rate of I atoms production increases with the HI flow rate for given NO and ClO₂ flow rate, but up to a certain limit only. With further increasing HI flowrate, the overall production rate of I atoms remains constant (see **Figs. 14** and **15**). A limited production of I atoms is apparently determined by the rate of atomic chlorine formation in the reaction system at the given flow rates of ClO₂ and NO. An increase in HI flow rate over this production rate of Cl atoms has apparently no effect on I atoms generation. Therefore the rate of I atoms production follows approximately the molar flow rate of HI up to a certain value from which the I atoms production rate is nearly constant (see **Figs. 14** and **15**). It was further found that the rate of I atoms production is higher at higher ClO₂ flow rate. For example, the production rate of about 50 μmol I/s was measured at 300 μmol ClO₂/s (see **Fig. 16**), whereas 37 μmol I/s only at 180 μmol ClO₂/s (see **Fig. 14**). These data relate to the same NO flow rate (180 - 190 μmol/s) through the injectors I#1 and I#2, and 200 μmol HI/s through the I#3. In the former case, the rate of Cl atoms production was apparently higher resulting therefore in a higher rate of I atom production. It follows from the modelling that the maximum of iodine atoms should be produced at NO/ClO₂ ratio equal to 2. From the comparison of curves in **Figs. 15** and **17** follows, however, that the I atoms production rate increases on decreasing this ratio from 2 to 1. This finding may be explained by a limiting rate of reactants mixing (the model assumes an instantaneous mixing). In the real system, reaction zones with an excess of NO (over ClO₂) are formed, where chlorine atoms (having very short lifetime) are produced (see the Report 0002). They may be recombined faster than are transferred into the HI stream. In the system with NO/ClO₂ ratio lower than 2, a formation of the zones with an excess of NO is suppressed and a loss of Cl atoms as well. This hypothesis is supported by the experiment, in which HI was injected through the injector I#2 and the second part of NO through the injector I#3. In this arrangement, HI could be distributed uniformly into the stream of ClO radicals flowing from the first injector, so that Cl atoms were formed (downstream the injector I#3) in the gas with an uniform concentration of hydrogen iodide. In this experiment (the ratio NO/ClO₂ = 1.4), the atomic I yield was extremely high - over 90 % (related to both ClO₂ and HI flowrate, respectively). The data presented in **Figs. 12** to **17** were measured with the longer cell (10 cm in length).

In the experiments where a new, shorter optical cell 11 (4.5 cm long and welded directly to the reactor) was used, the production rate of I atoms estimated by the diode probe laser was rather high (see **Fig. 18**)

3.2.3. Conclusions from experimental investigation

The performed experimental investigation confirmed the possibility to generate atomic iodine by the suggested chemical method based on mixing of gaseous reactants in the pressure and flow conditions applicable to COIL. In the study of the reaction kinetics of this process, the following effects were found:

- The production rate of atomic iodine increases with HI flow rate up to some limit, given apparently by the rate of chlorine atoms production.
- The production rate of atomic iodine increases with decreasing ratio of NO/ClO₂ from 2 to 1. This finding, which does not coincide with the results of modelling, is explained by the limited rate of mass transfer between the streams of generated Cl atoms and HI molecules which results in larger loss of Cl atoms at the stoichiometric ratio of ClO₂ : NO (1 : 2).
- The above assumption was also verified in the experiment where streams of HI + ClO radicals were mixed prior to Cl atoms formation, which resulted in very high yield of I atoms (over 90 % related to the reactants flow rate).
- The flowrate of atomic iodine determined by the diode probe laser diagnostics was lower than the overall flowrate of atomic iodine determined from the concentration of molecular iodine after I atoms recombination. This finding is in qualitative agreement with the modelling results. It reflects the fact of the fast decrease in I atoms concentration along the gas flow in the detection cell of the diode probe laser diagnostics. The average concentration found experimentally is much higher than corresponds to the theory, which is explained by the mass transfer limitation.
- It can be concluded from the results of modelling and experiments obtained on the small scale experimental device that in an application of this method in the COIL, iodine atoms must be generated as close as possible to the critical nozzle plane.

Appendix I

Controlling sequences

START PROGRAM

START OF ADJUSTING SECTION

LASER BYPASS OPENING

THROTTLE VALVE ADJUSTING

BHP PUMP ON

BHP PUMP FREQUENCY SETTING

PRIMARY He VALVE OPENING

SECONDARY He FLOW RATE ADJUSTING

I₂ FLOW RATE ADJUSTING ON ZERO

I₂ BYPASS OPENING

I₂ VALVE OPENING

I₂ BYPASS CLOSING

END OF ADJUSTING SECTION

START OF LASER OPERATION (can be repeated)

I₂ FLOW RATE ADJUSTING ON DESIRED VALUE

PRIMARY He INTO Cl₂ VALVE OPENING

Cl₂ VALVE OPENING

GATE VALVE OPENING

LASER BYPASS CLOSING

PRIMARY He DOWN STREAM JSOG VALVE OPENING

LASER BYPASS OPENING

GATE VALVE CLOSING

Cl₂ VALVE CLOSING

PRIMARY He INTO Cl₂ VALVE CLOSING

PRIMARY He VALVE CLOSING

END OF LASER OPERATION

STOPPING SEQUENCE

STOP PROGRAM

Appendix II

Determination of HI concentration

Hydrogen iodide in the gaseous mixture discharged from the gas cylinder was absorbed (during 30 s) in 200 ml of distilled water. From 200 ml of this solution, 20 ml was titrated by 0.05 M AgNO₃ with potassium chromate used as the indicator. The percentage HI concentration in the gas mixture was calculated by

$$c_{\text{HI}} = (V_{\text{AgNO}_3} \times 0.05 \times 200 \times 100) / (n \times 20 \times 30) ,$$

where V_{AgNO_3} is the AgNO₃ consumption, n is the molar flow rate of gas mixture calculated from the flowmeter reading.

Examples of chemical analysis of the gaseous mixture HI + N₂

- a) A content of HI in newly prepared mixture of HI + N₂ was 7.5 % according to readings on the pressure meter.
- b) A content of HI after 29 days of the gas cylinder standing (without any shaking the vessel) was 3.5 %.
- c) A content of HI after 2 min.'s shaking the gas cylinder was 6.2 and 6.3 %.
- d) A content of HI after 5 days' gas cylinder standing was 4.6 and 5.3 %.
- e) After shaking the gas cylinder for 5 min, the content of HI was again 6.4 and 6.3 %.
- f) After 3 hour's standing the gas cylinder, the gas contained 5 % HI
- g) After 8 days' standing the gas cylinder and 3 min.'s shaking, the HI content was 6.3 %.

It follows from this experimental experience that the gas cylinder with HI + N₂ mixture must be shacked if it stands without using for more than several tens minutes.

4. References

- [1] S.-O. Kwon, T.-S. Kim, S.-H. Kim, Y.-D. Choi, Y.-S. Lee, Y.-S. Park, H.-S. Kim, Ch.-J. Kim, GCL/HPL conference, Florence 2000, Proc. SPIE Vol. **4184**, p.107, 2000.
- [2] J. Arnold, K.D. Foster, D.R. Snelling and R.D. Suart, IEEE J. Quant. Electr. **QE-14** (1978) 293.

- [3] K. Bergmann and C.B. Moore, *J. Chem. Phys.* **63** (1975) 643.
- [4] E. Endo, D. Sugimoto, H. Okamoto, K. Nanri, T. Uchiyama, S. Takeda and T. Fujioka, *Jap. J. Appl. Phys.* **39** (2000) 468.
- [5] P.P. Bemand, M.A.A. Clyne and R.T. Watson, *J.C.S. Faraday Trans. I* **69** (1973) 1356.
- [6] H.van den Bergh and J. Troe, *J. Chem. Phys.* **64** (1976) 736.
- [7] P.G. Ashmore and J. Chanmugan, *Trans Faraday Soc.* **49** (1953) 270.
- [8] D.L. Carroll, *AIAA J.* **33** (1995) 1454.
- [9] Yu.A. Kulagin, L.A. Shelepin and V.N. Yarygina, *Trudy FIAN* **218** (1994) 166.
- [10] J.P. Singh, J. Bachar, D.W. Setser and S. Rosenwaks, *J. Phys.Chem.* **89** (1985) 5347.
- [11] K.H. Becker, W.Groth and U. Schurath, *Chem. Phys. Lett.* **8** (1971) 259.
- [12] A.T. Pritt and R.D. Coombe, *J. Chem. Phys.* **65** (1976) 2096.
- [13] D.H. Burde and R.A. McFarlane, *J. Chem. Phys.* **64** (1976) 1850.
- [14] W. Schneider, G.K. Moortgat, G.S. Tyndall and J.P.Burrows, *J.Photochem. Photobiol.A: Chemistry*, **40** (1987) 195.

5. Acknowledgement

The investigators are very grateful to the USAF European Office for Research and Development (EOARD) for the support of this work. We thank to Dr. Martin Stickley and Dr. Alexander Glass, the former and present Program Managers, Lasers and Photonics at the EOARD, for their assistance with this contract.

We have benefited very much during the work on the contract from discussions with Dr. Gordon Hager, Dr. Brian Anderson, Dr. Ralph Tate and Dr. Harro Ackermann from the US AFRL at the Kirtland Base, NM.

6. Project Cost

1. Expendable supplies and materials:		\$4,830
Gases and chemicals:		\$2,950
- HI synthesis and analysis	\$1,600	
- Helium	\$800	
- Other chemicals (N ₂ , NO, Cl ₂ , KOH, H ₂ O ₂)	\$550	
Office supplies:		\$300
Constructional materials:		\$500
Software for data acquisition and device control	\$550	
Cost of repairing the vacuum elements (valves, pumps)	\$530	
2. Equipment purchased:		\$3,450
- Spec. valves and pressure sensors for aggressive medium	\$2,300	
- Computer + monitor (for diode probe diagnostics)	\$1,150	
2. Travel cost:		\$1,700
- GCL/HPL conference, Italy (part of total expend of 3 particip.)	\$1,700	
4. Publications, Reports preparation, Literature purchased:		\$120
5. Overhead charges:		\$2,500
6. Labor: rewards + tax to the state (approx. 37 % of reward): ¹		\$12,400

	Planned Paid		
Dr Jarmila Kodymová (PI), senior sci.	\$3,000	\$2,200 + \$800 (tax) =	\$3,000
Dr Otomar Špalek (PI), senior sci.	\$3,000	\$2,200 + \$800 =	\$3,000
Vít Jirásek, PhD, junior sci.	\$1,500	\$1,500 + \$550 =	\$2,050
Miroslav Čenský, PhD student	\$1,000	\$1,000 + \$400 =	\$1,400
Dipl Ing Jan Kuželka, engineer-spec.	\$400	\$750 + \$280 =	\$1,030
4 Technicians	\$1,600	\$1,400 + \$520 =	\$1,920

Total project cost **\$25,000**

¹ Note: The rewards represent the extra money to regular salaries paid to all listed people by the Institute of Physics (the Government). The salaries are approximately on this level: a net salary (reduced by the tax) of senior scientists is in average of \$400/month, i.e. \$2.4/hr, junior scientists and engineers of \$270/month, i.e. \$1.8/hr, and technicians \$1,4/hr.

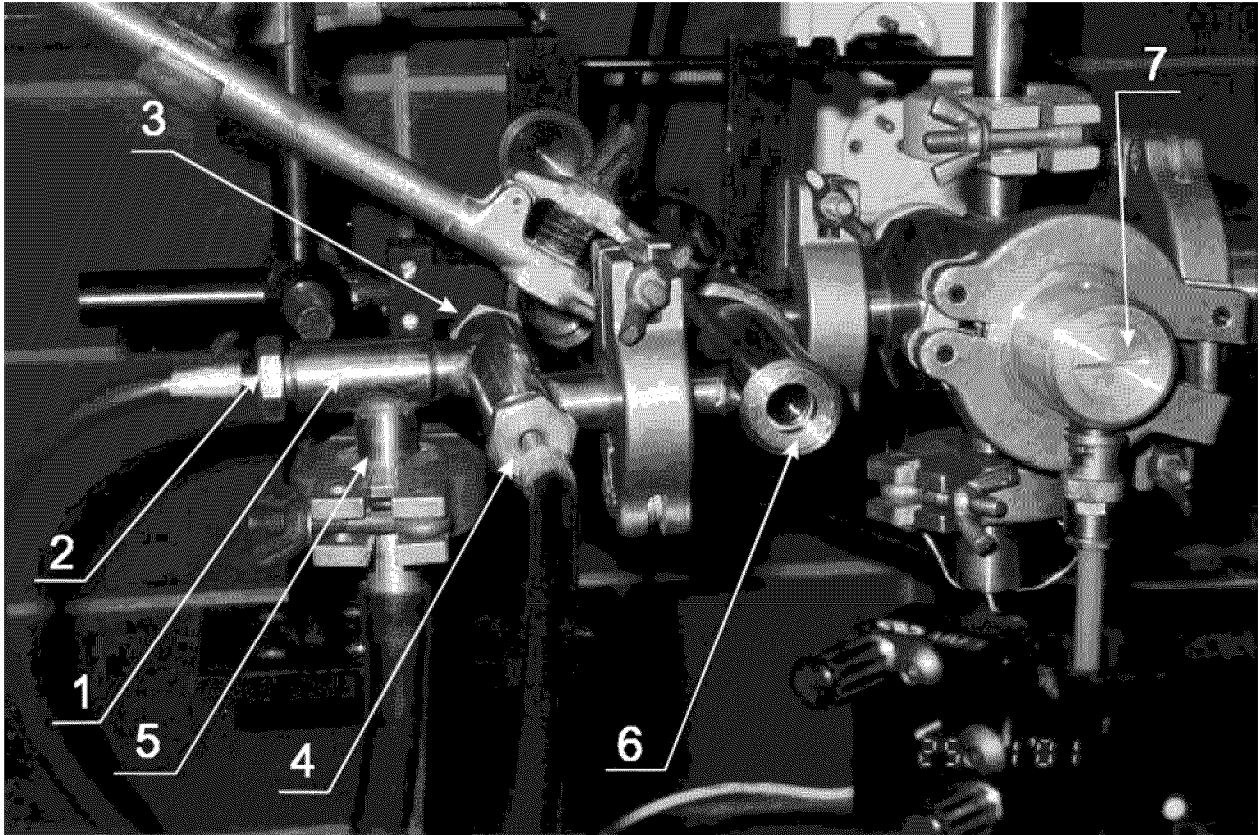


Photo 1. Small experimental device for atomic iodine generation

1 – reactor, 2 – injector I#1, 3 – injector I#2, 4 – injector I#3, 5 – ClO_2 input,
6 – optical cell for atomic iodine detection by diode probe diagnostics,
7 – optical detection of I_2 molecules by Argon ion laser (in the first cell).

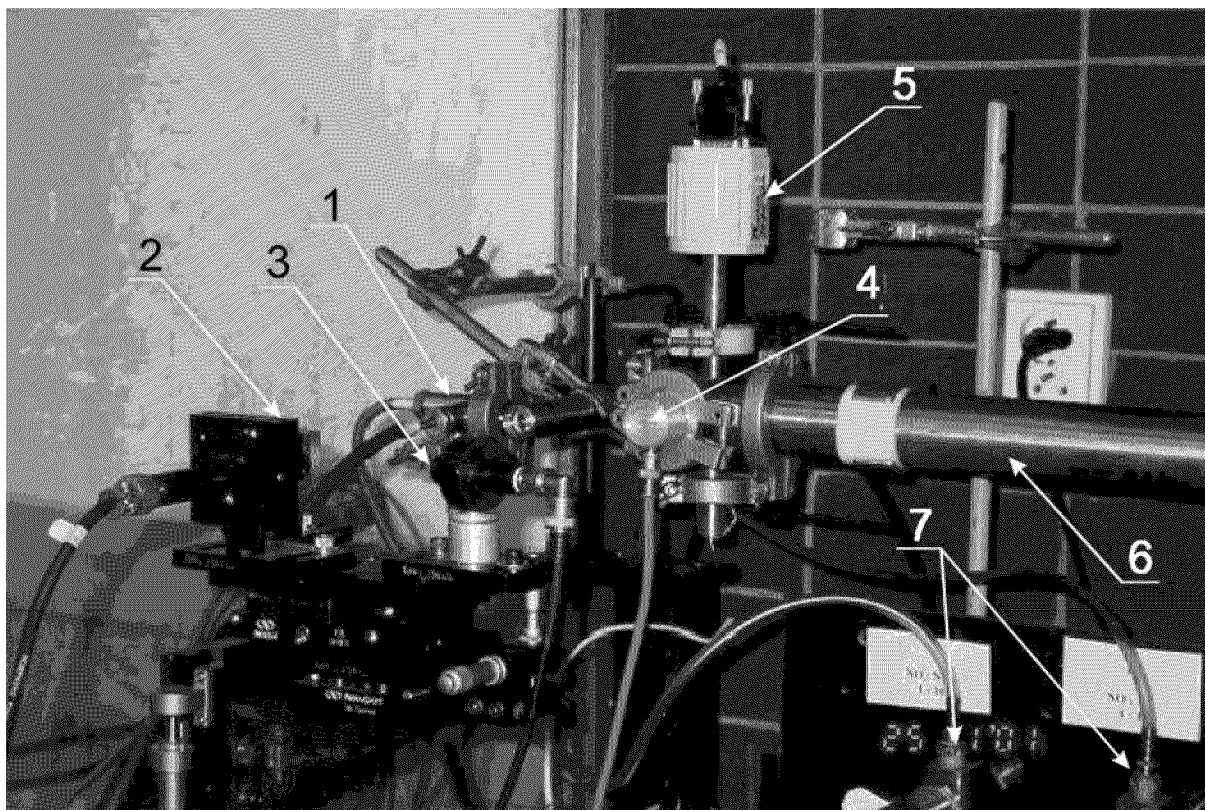


Photo 2. Small experimental device for atomic iodine generation and detection

1 – reactor, 2 – beam of diode laser, 3 – detector of diode laser beam, 4 – optical detection of I₂ molecules by Argon ion laser (in the first cell), 5 – pressure gauge, 6 – tube between the first and second I₂ detection cell, 7 – flow meters for reactants with measuring orifices.

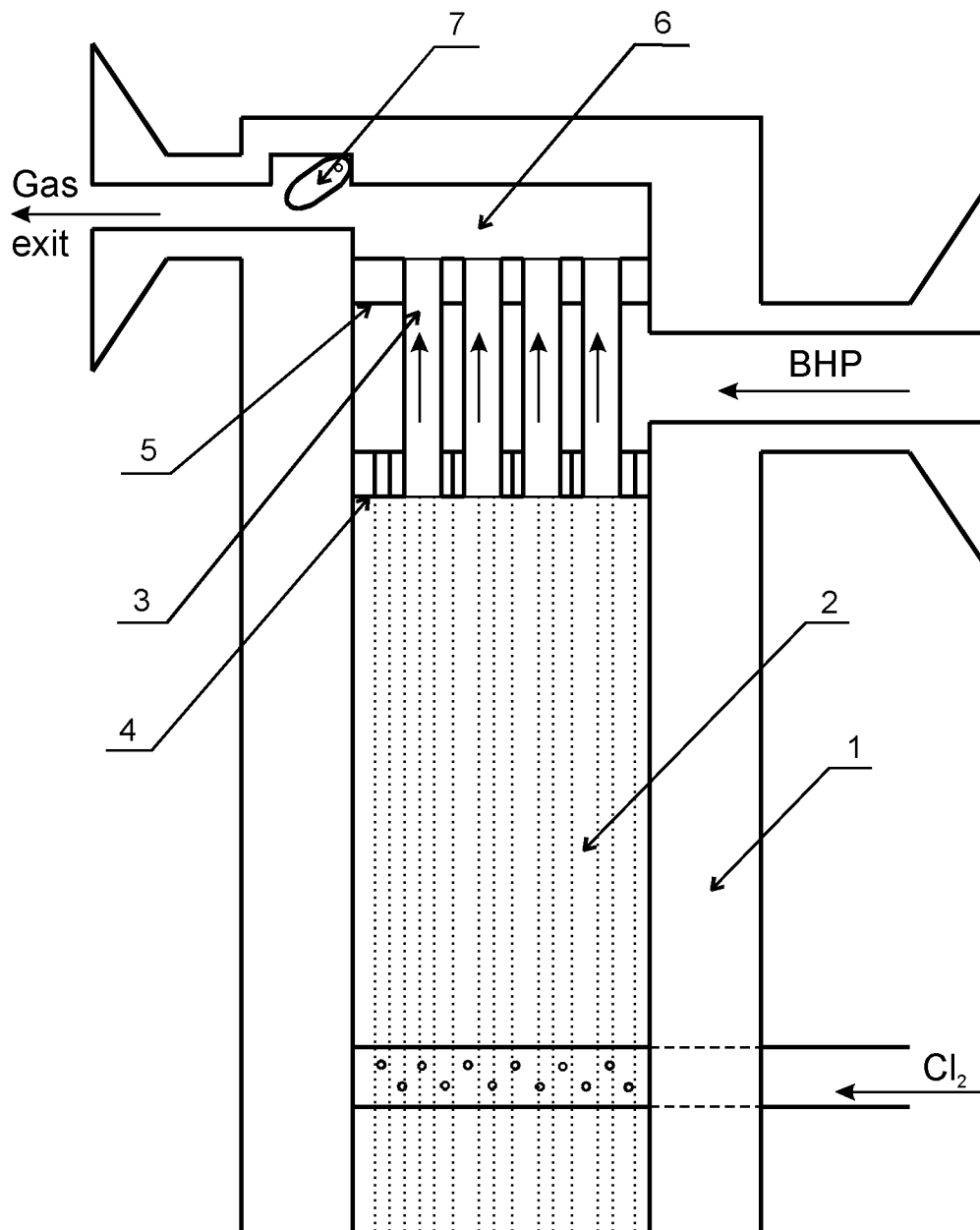


Fig 1. Scheme of the jet SOG with vertical gas exit (arrows).

- 1 – generator body, 2 – g/l reactor, 3 – gas exit channels (made of metal tubes),
- 4 – BHP injector, 5 – plate dividing BHP cavity and gas space (with filler in some case),
- 6 – gas space, 7 – throttle valve

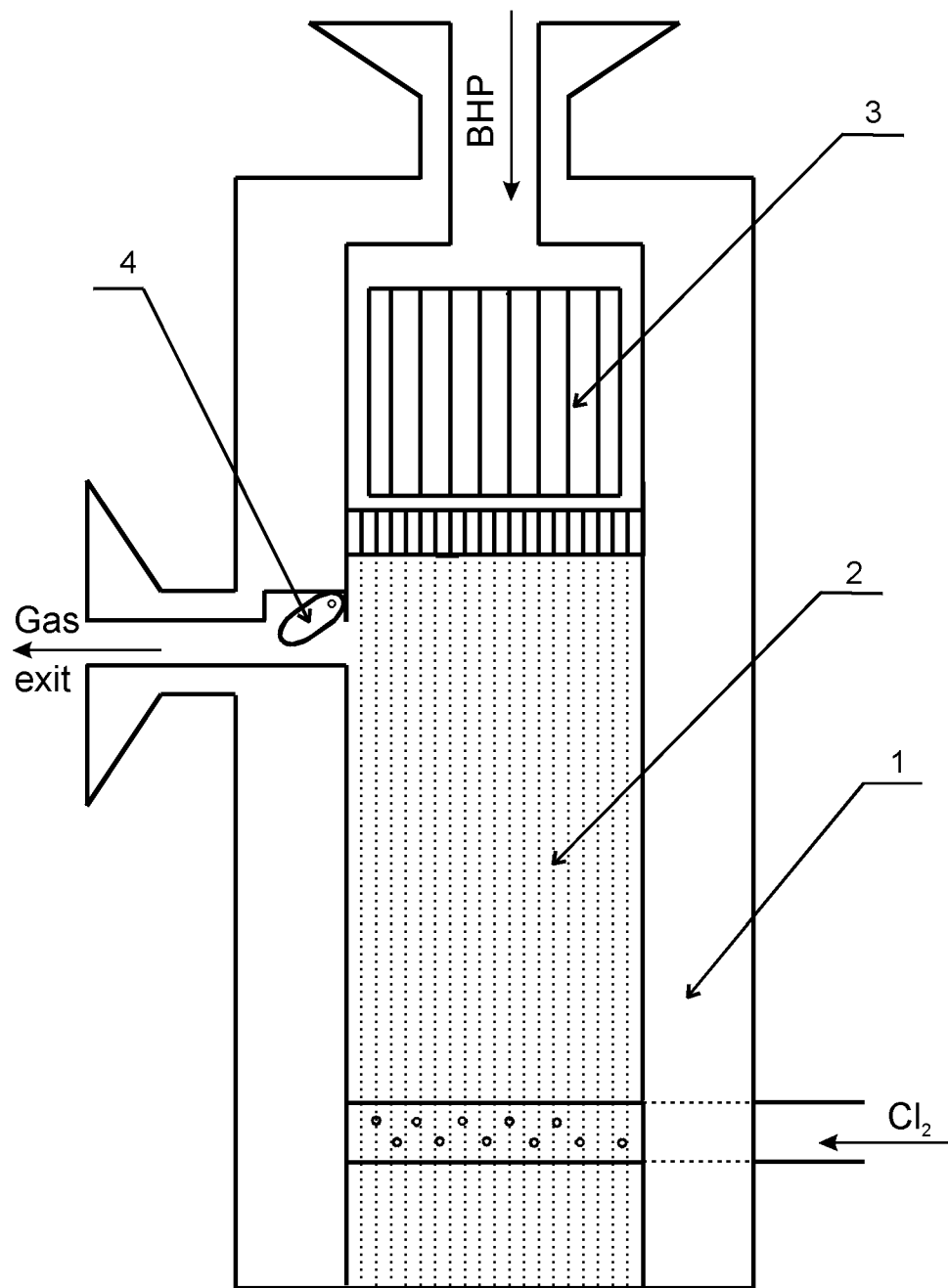


Fig 2. Scheme of the jet SOG with horizontal gas exit and installed BHP directors in space above BHP injector

1 – generator body, 2 – BHP jets, 3 – BHP directors, 4 – throttle valve

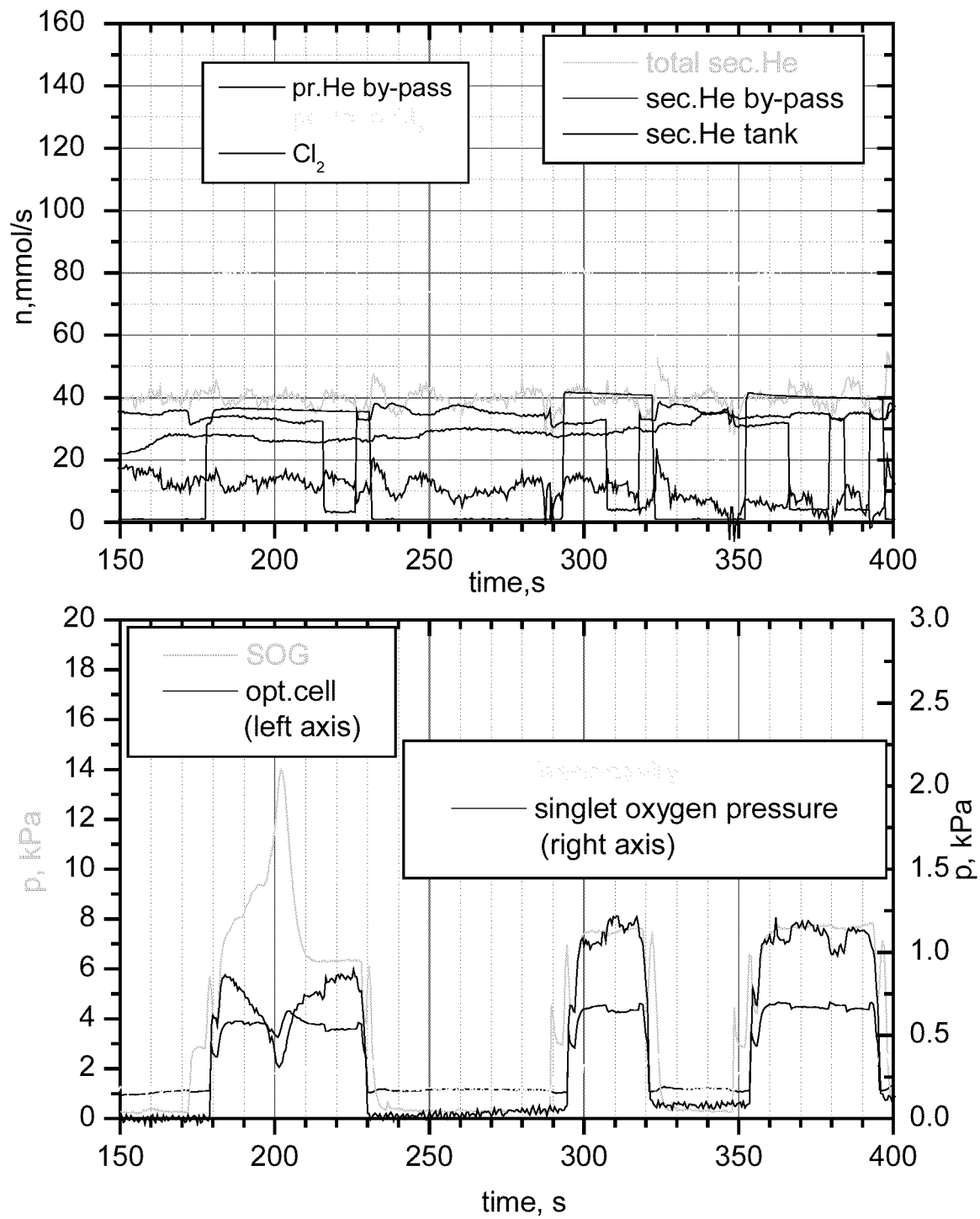


Fig. 3a,b. COIL measurement. Time course of flowrates of primary and secondary gases (upper graph), total pressures in singlet oxygen generator, subsonic channel, laser cavity and partial pressure of singlet oxygen (bottom graph).

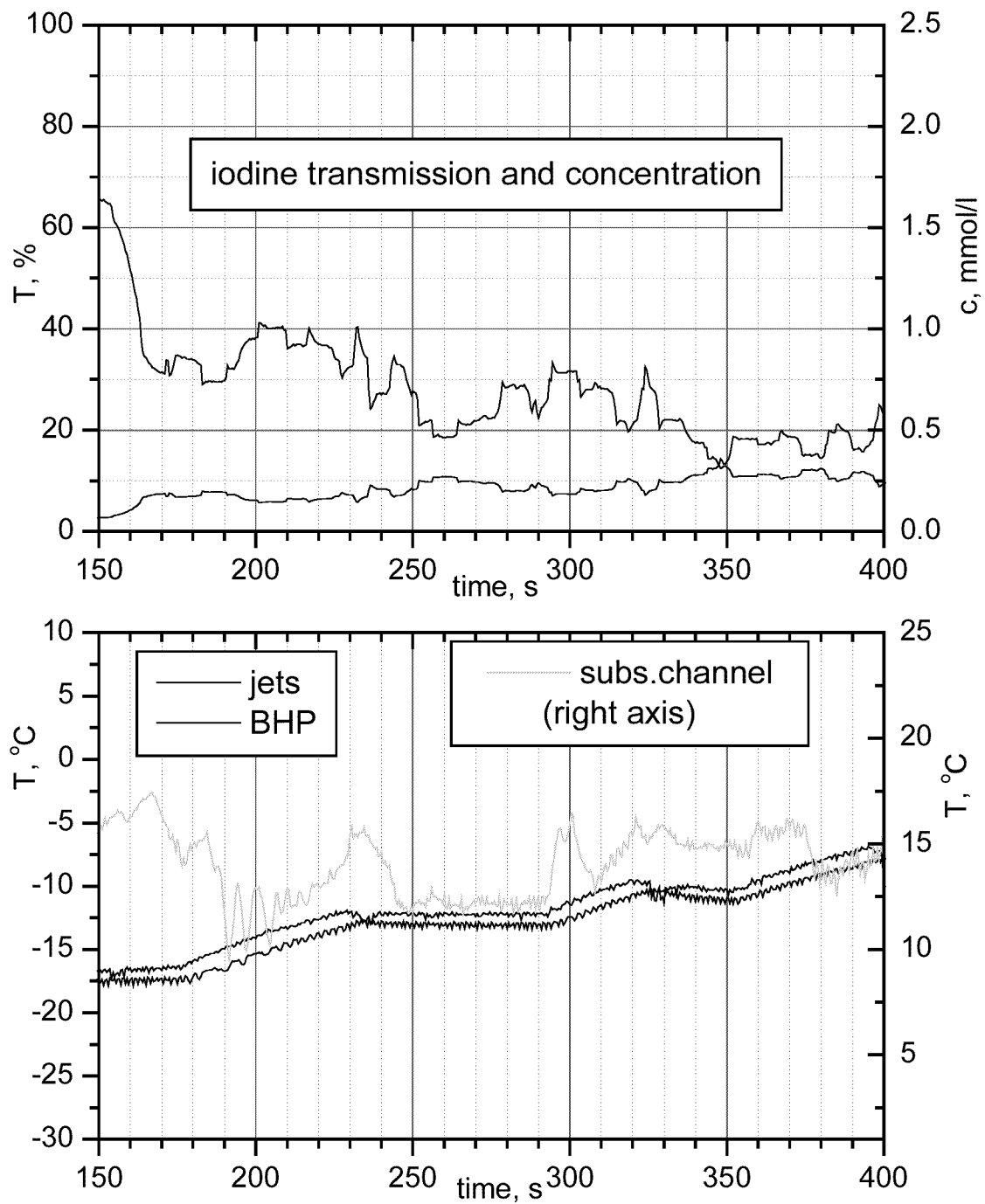


Fig. 4a,b. COIL measurement. Time course of transmission of the light at 488 nm by iodine vapor and calculated iodine concentration (upper graph). Time course of temperatures of BHP jets, BHP reservoir and subsonic channel (bottom graph).

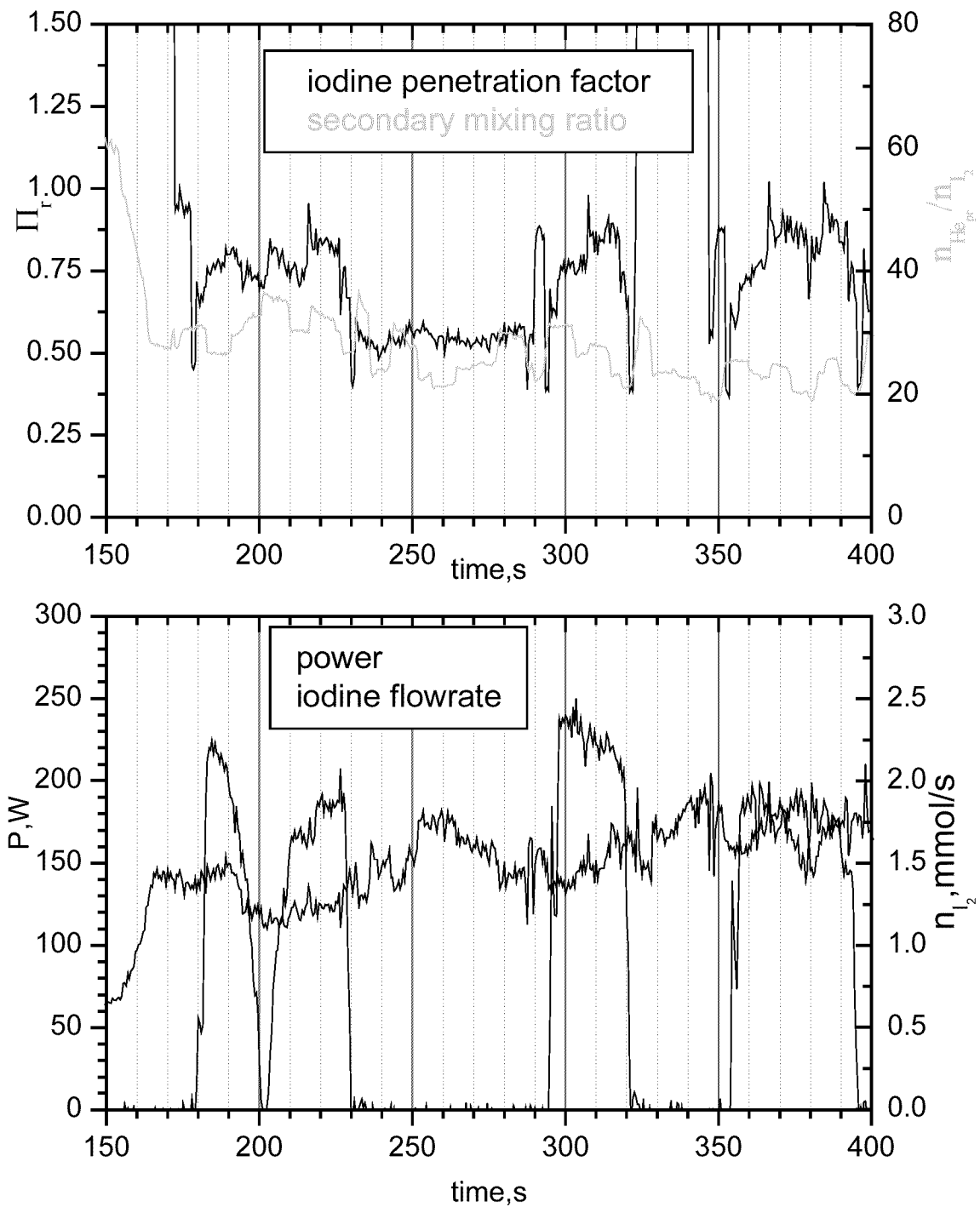


Fig.5a,b. COIL measurement. Time course of penetration factor of secondary stream, and ratio between secondary helium flowrate and iodine flowrate (upper graph). Time course of laser power and calculated iodine flowrate (bottom graph).

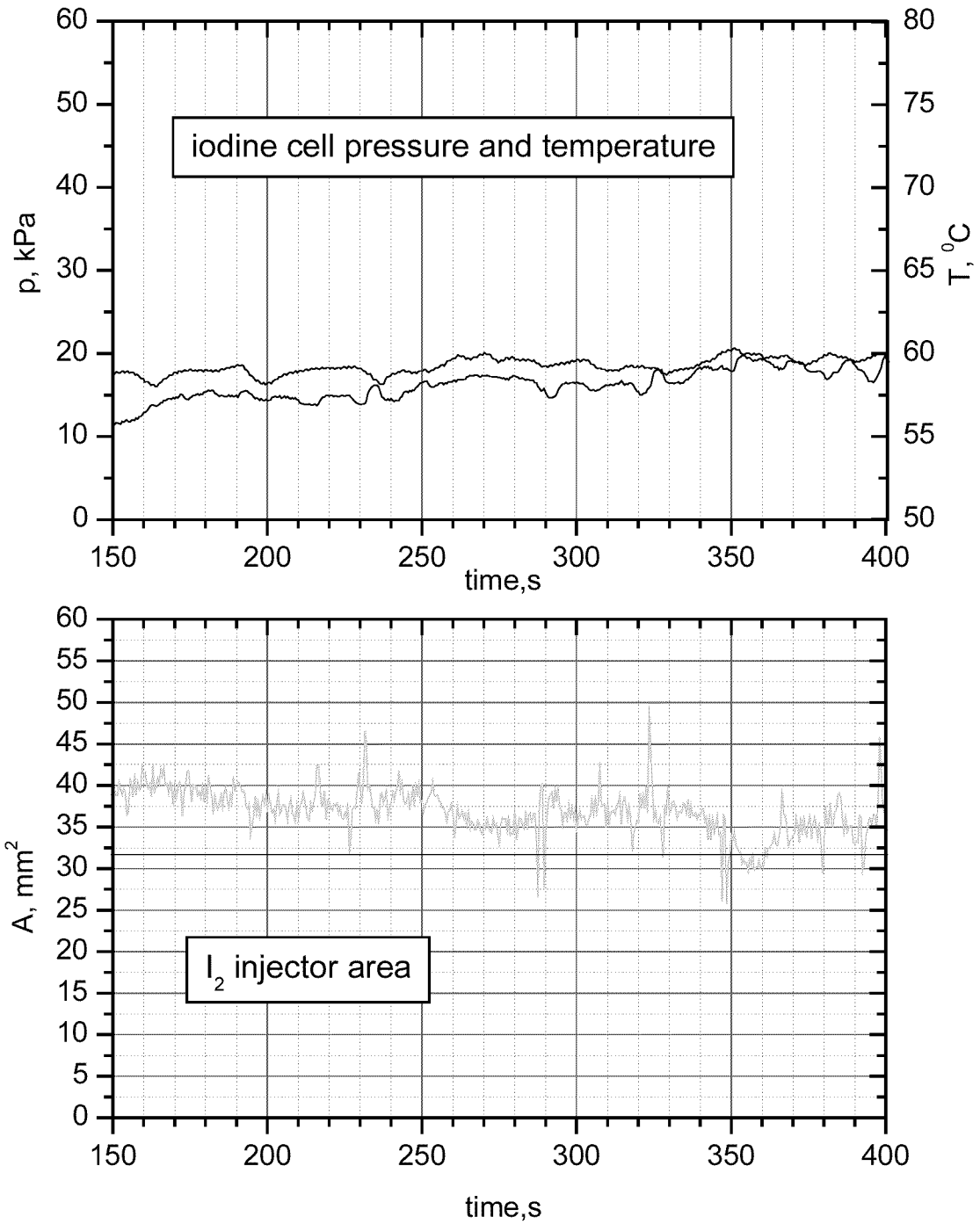


Fig. 6a,b. COIL measurement. Time course of the pressure in iodine detection cell (upper graph). Time course of the free cross-section area of openings in the I_2 injector (bottom graph).

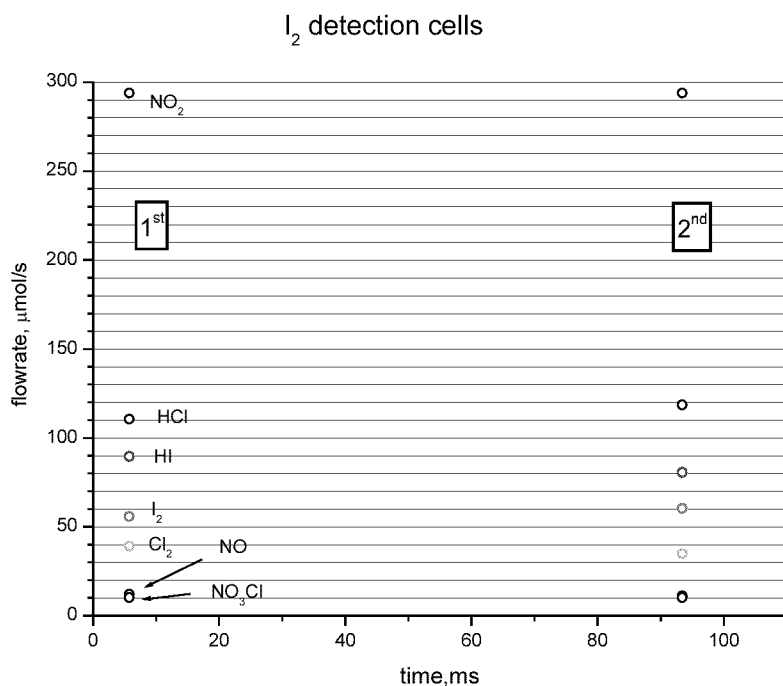
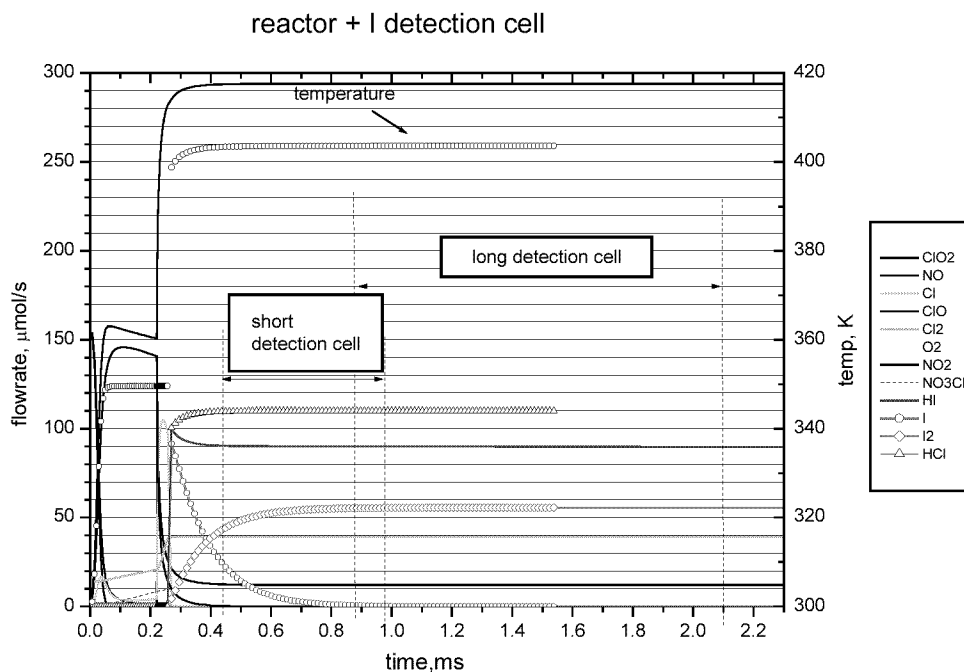


Fig. 7. Modeling results: time course of molar flowrates of reactants and products, and adiabatic temperature from the moment of the first NO injection. The location of two versions of detection cell for atomic iodine diagnostics by the diode probe laser is shown in the upper graph and two detection cells for the I₂ detection by Ar laser are shown in the bottom graph. Initial flowrates: ClO₂ : NO(I) : NO(II) : HI = 160 : 160 : 160 : 200 (in $\mu\text{mol/s}$).

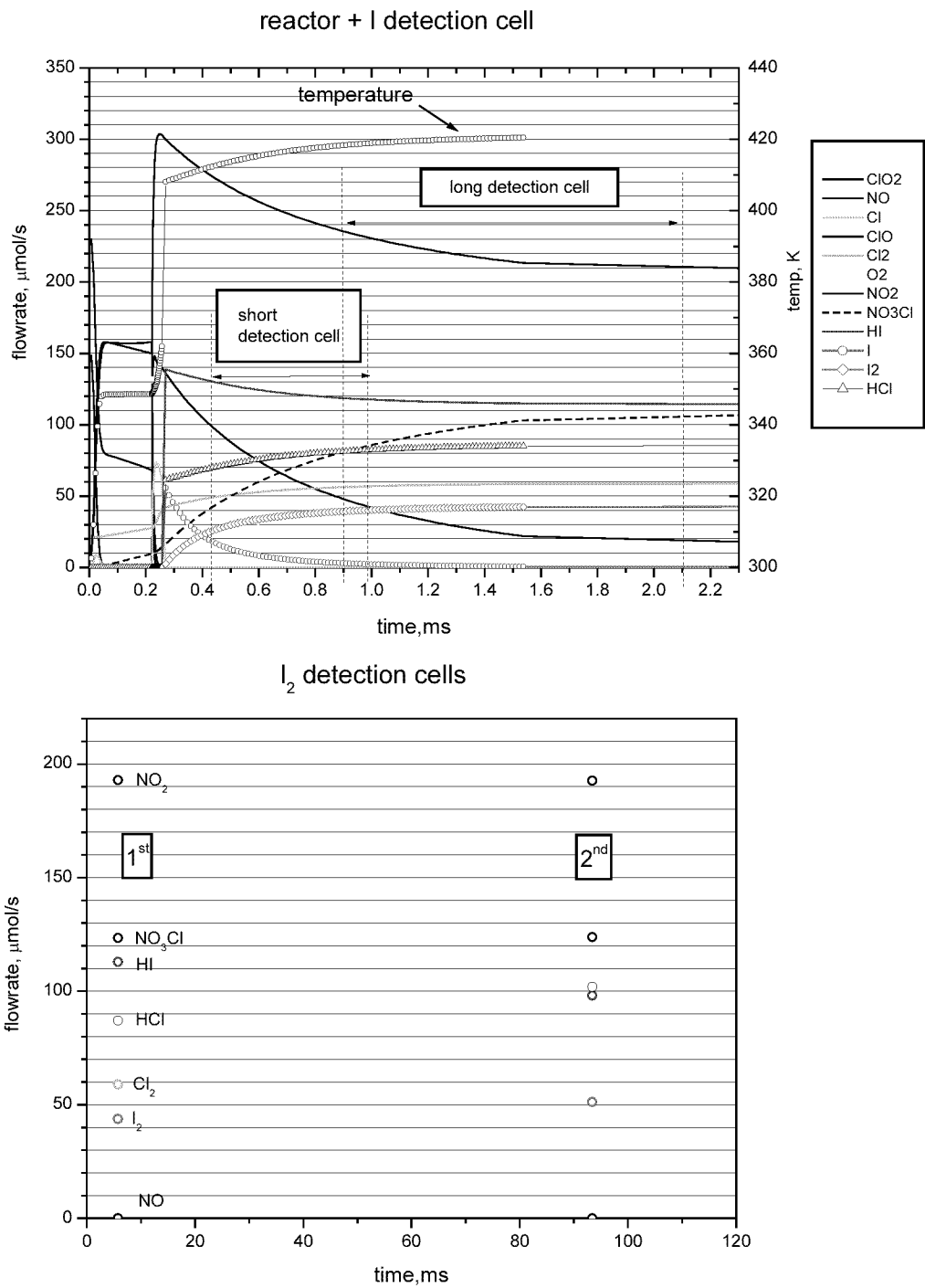


Fig. 8. Modeling results – key as in Figure 7.

Initial flowrates: ClO_2 : NO(I) : NO(II) : HI = 240 : 160 : 160 : 200 (in $\mu\text{mol/s}$).

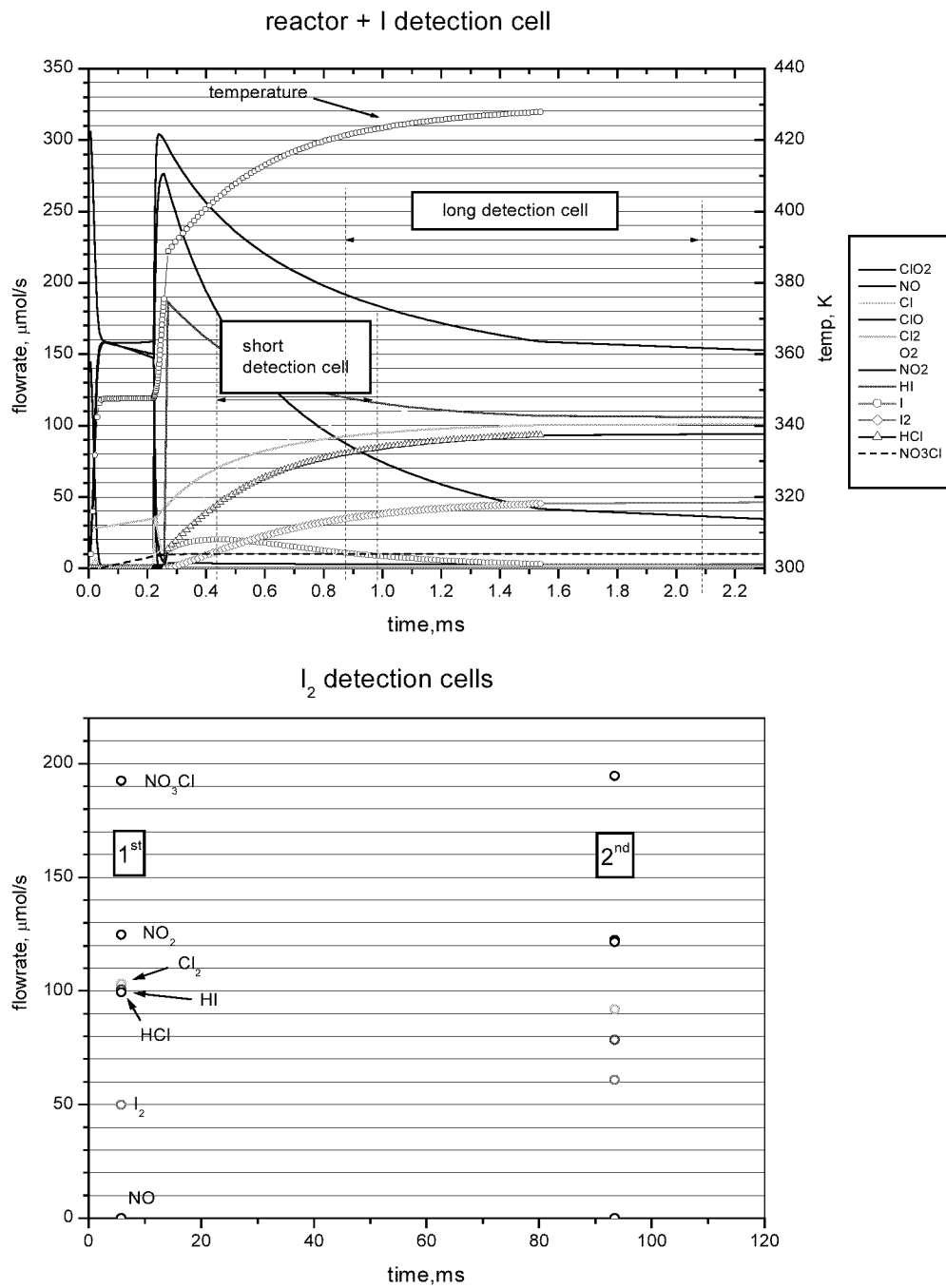


Fig. 9. Modeling results – key as in Figure 7.

Initial flowrates: ClO_2 : NO(I) : NO(II) : HI = 320 : 160 : 160 : 200 (in $\mu\text{mol/s}$).

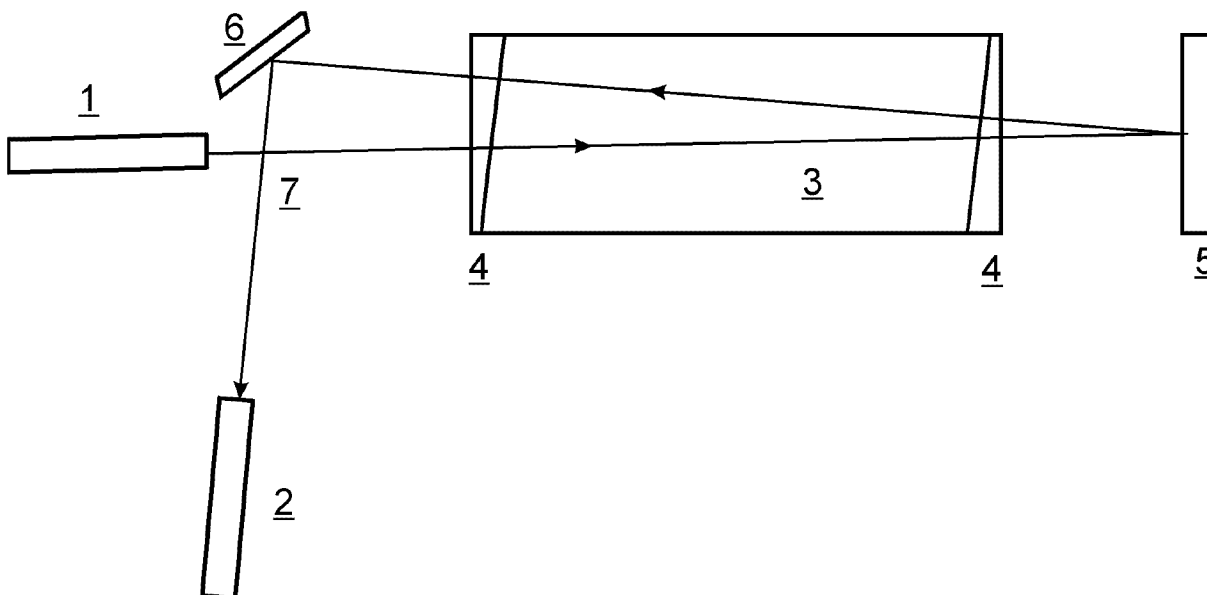


Fig. 10. Scheme of atomic iodine detection by diode laser. 1- probe laser emitter, 2 - detector, 3 - optical cell, 4 - wedge glass, 5, 6 - mirrors, 7 - probe beam

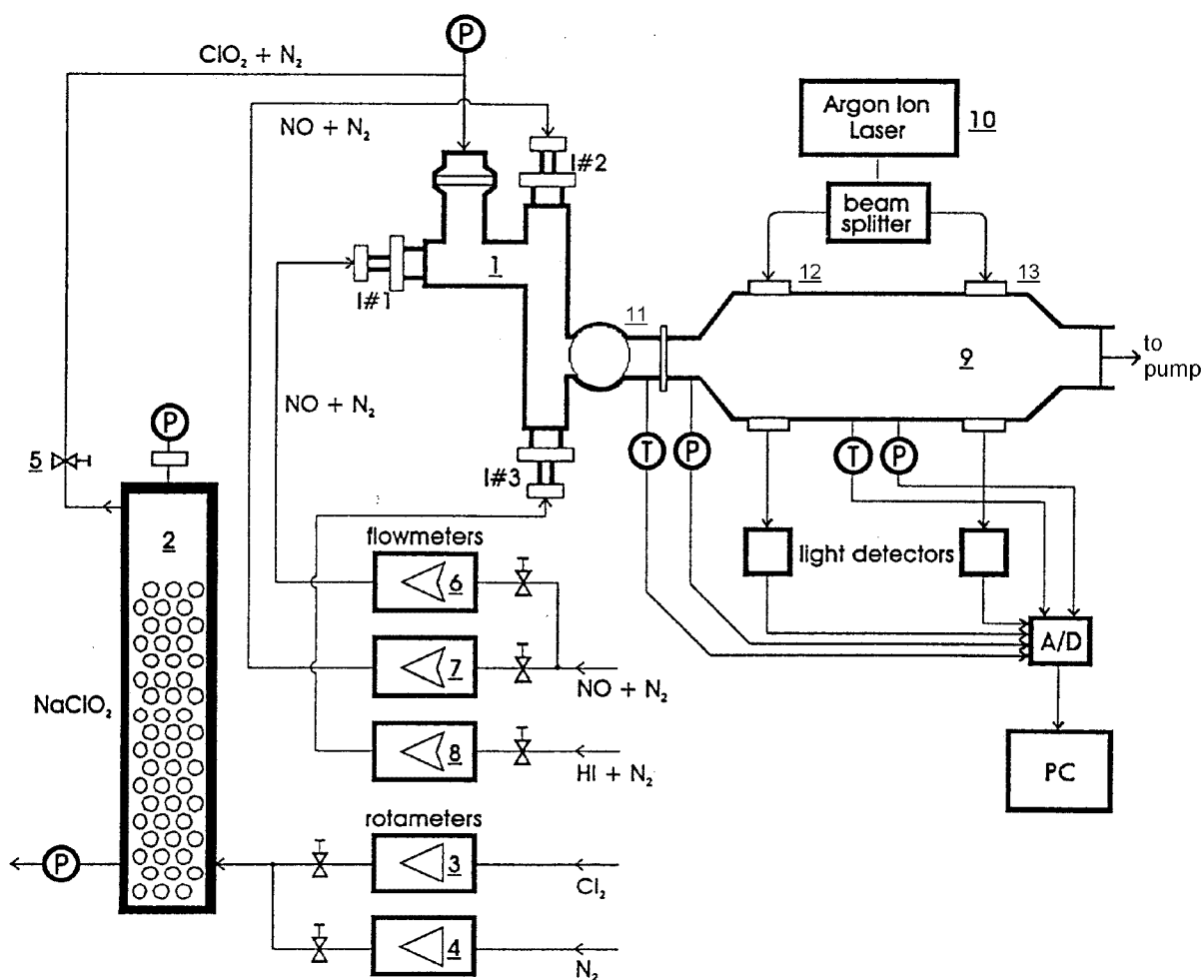


Fig. 11. Scheme of small-scale device for atomic iodine generation. 1 – flow chemical reactor, 2 – column generator of ClO_2 , 3,4 – rotameters, 5 – valve, 6, 7, 8 – flowmeters, 9 – diagnostics cell, 10 – Argon ion laser, 11 – optical cell for diode laser, 12, 13 – optical cells for Argon ion laser

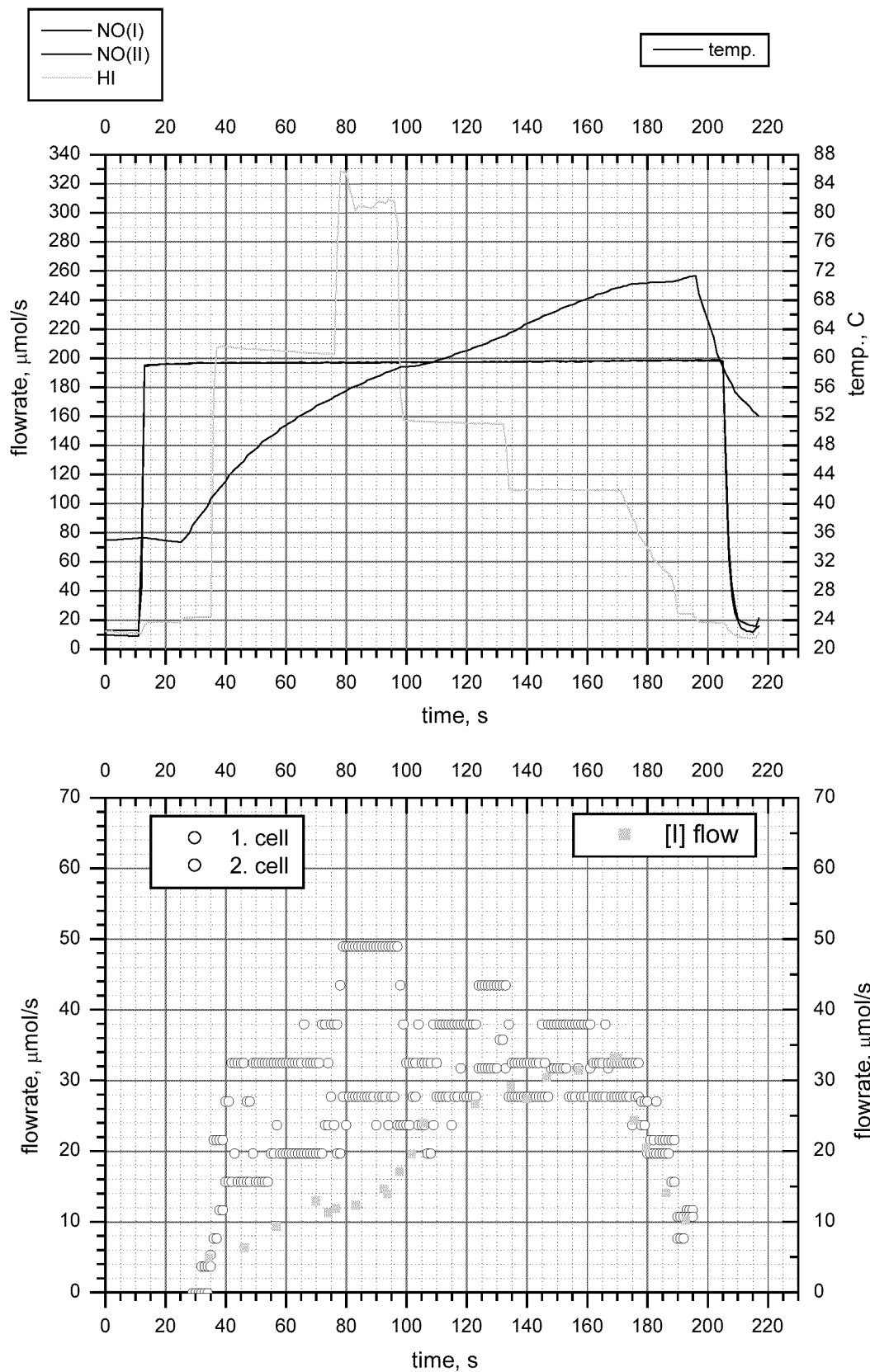


Fig. 12a,b. Measured time course of input flowrates of reactants and iodine flowrate for $300 \mu\text{mol ClO}_2/\text{s}$. Iodine flowrate is calculated from the concentration measured by the diode probe laser (green symbols) and from the molecular iodine concentrations measured by the Ar-ion laser multiplied by two (blue and red symbols).

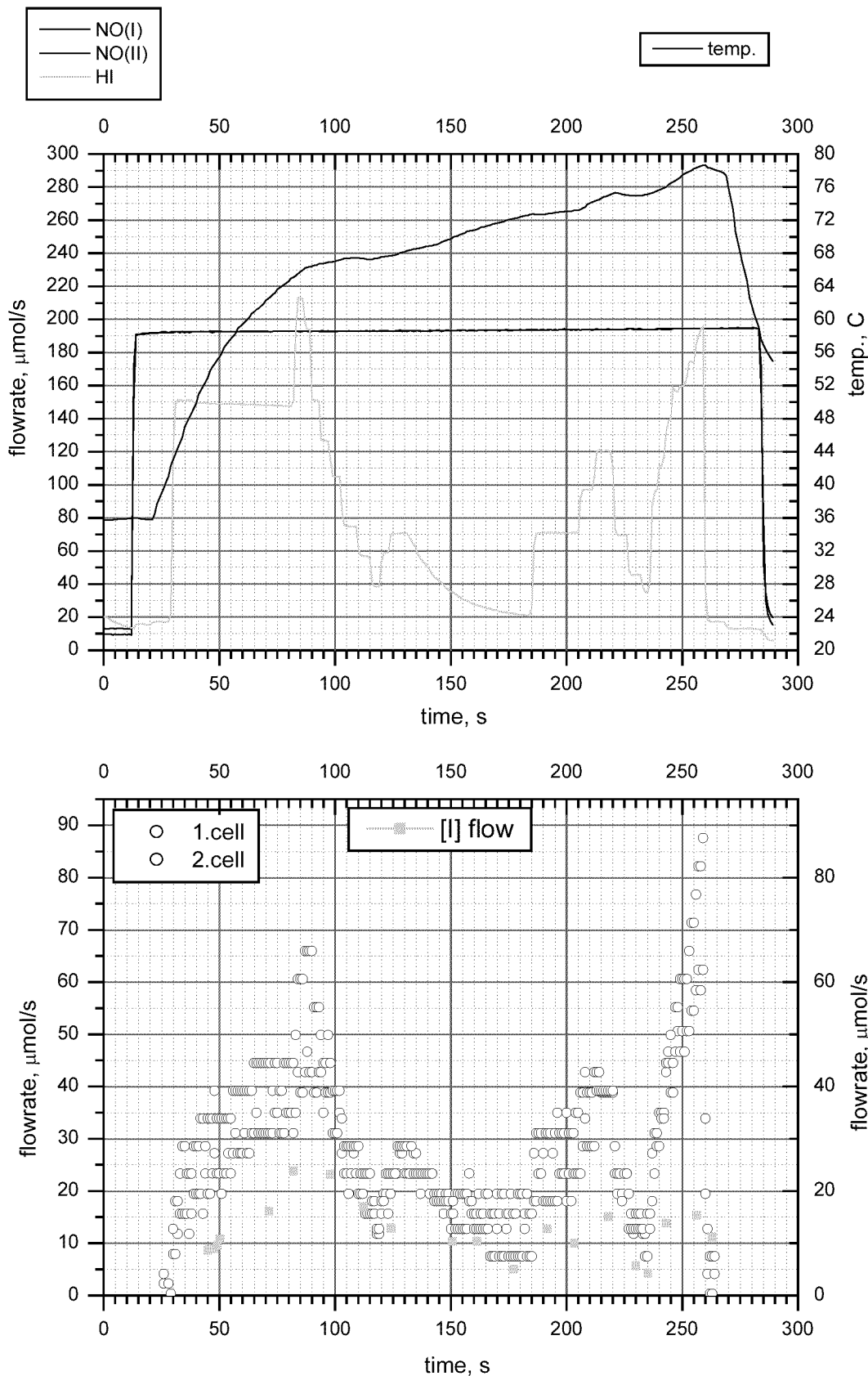


Fig. 13a,b. Measured time course of input flowrates of reactants and iodine flowrate for $269 \mu\text{mol ClO}_2/\text{s}$. Key as in Figure 12.

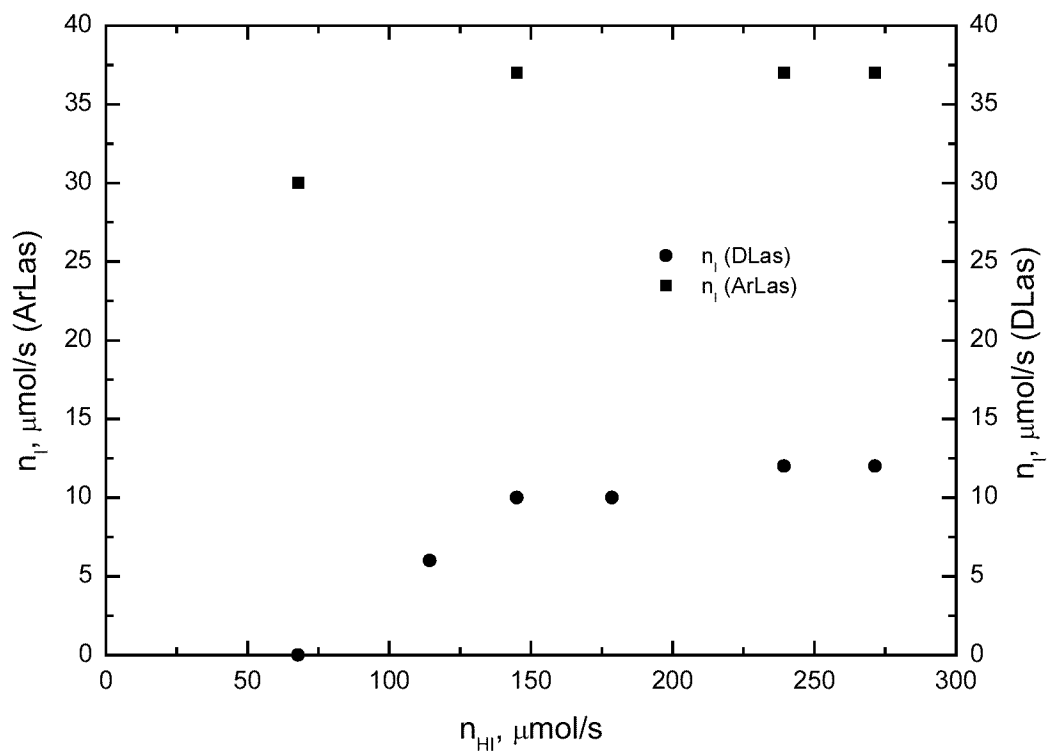


Fig.14. Atomic iodine flowrate as a function of the initial HI flowrate measured by the diode probe laser (red points) and Ar ion laser (black points). The latter values taken as a double value of measured I_2 flowrate.
Initial flowrates: 181 $\mu\text{mol ClO}_2/\text{s}$, 175 $\mu\text{mol NO(I)}/\text{s}$ and 185 $\mu\text{mol NO(II)}/\text{s}$.

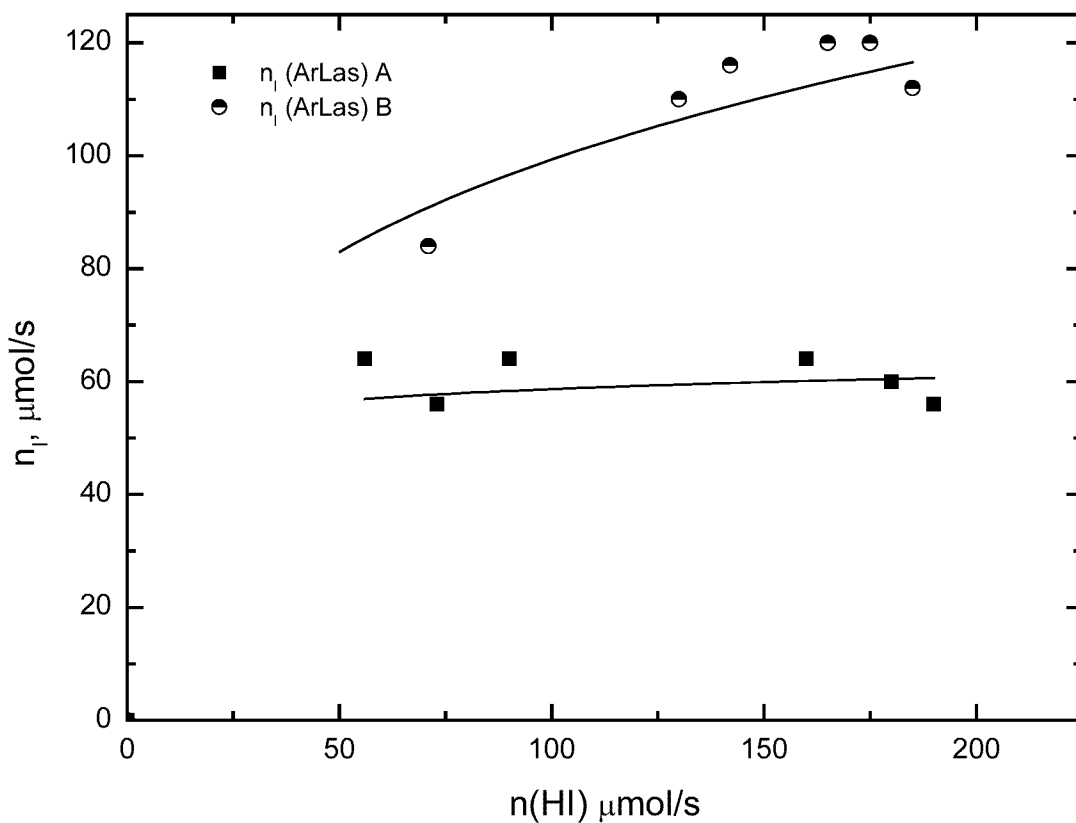


Fig. 15. Atomic iodine flowrate as a function of the initial HI flowrate – key as in Figure 14.
 Initial flowrates: 197 $\mu\text{mol ClO}_2/\text{s}$, 85 $\mu\text{mol NO(I)}/\text{s}$, and 85 $\mu\text{mol NO(II)}/\text{s}$ (black symbols); 197 $\mu\text{mol ClO}_2/\text{s}$, 137 $\mu\text{mol NO(I)}/\text{s}$, and 145 $\mu\text{mol NO(II)}/\text{s}$ (red symbols).

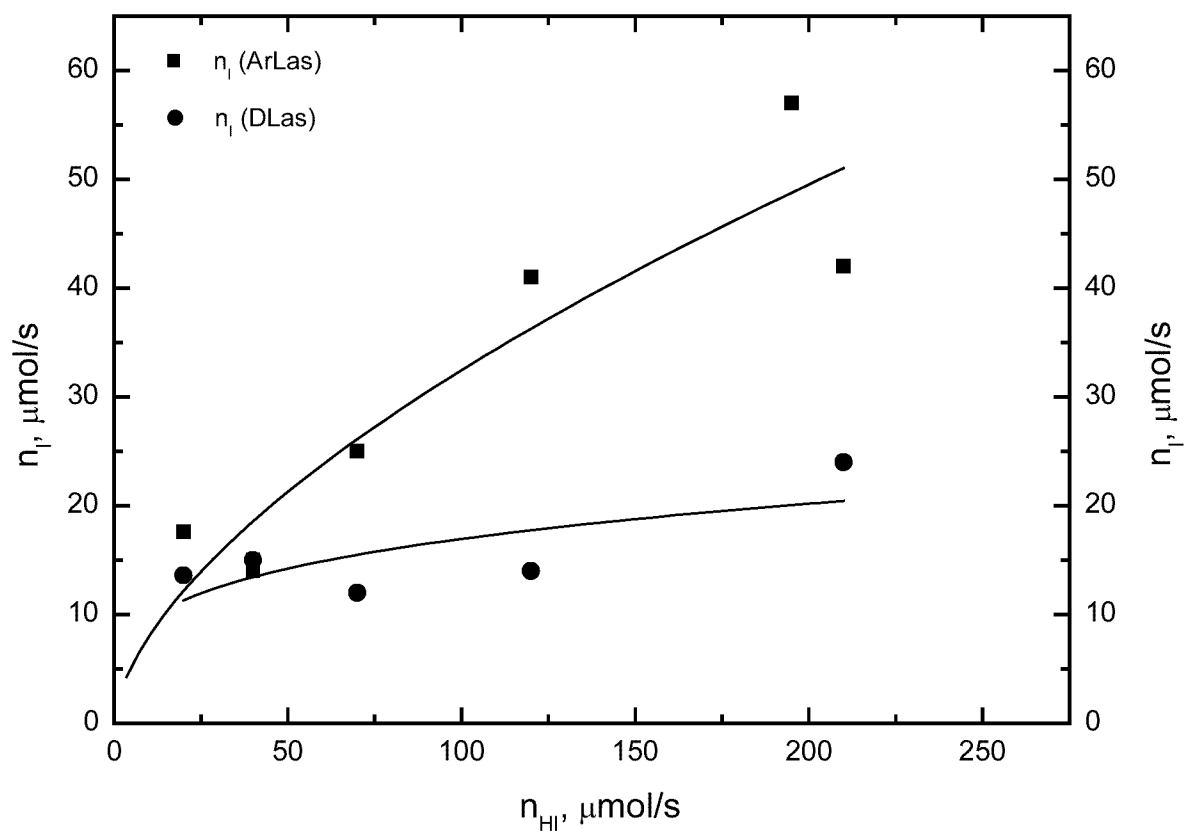


Fig.16. Atomic iodine flowrate as a function the initial HI flowrate measured in the first optical cell for two flowrates of NO(I+II).
Initial flowrates: 300 $\mu\text{mol ClO}_2/\text{s}$, 190 $\mu\text{mol NO(I)}/\text{s}$, and 190 $\mu\text{mol NO(II)}/\text{s}$.

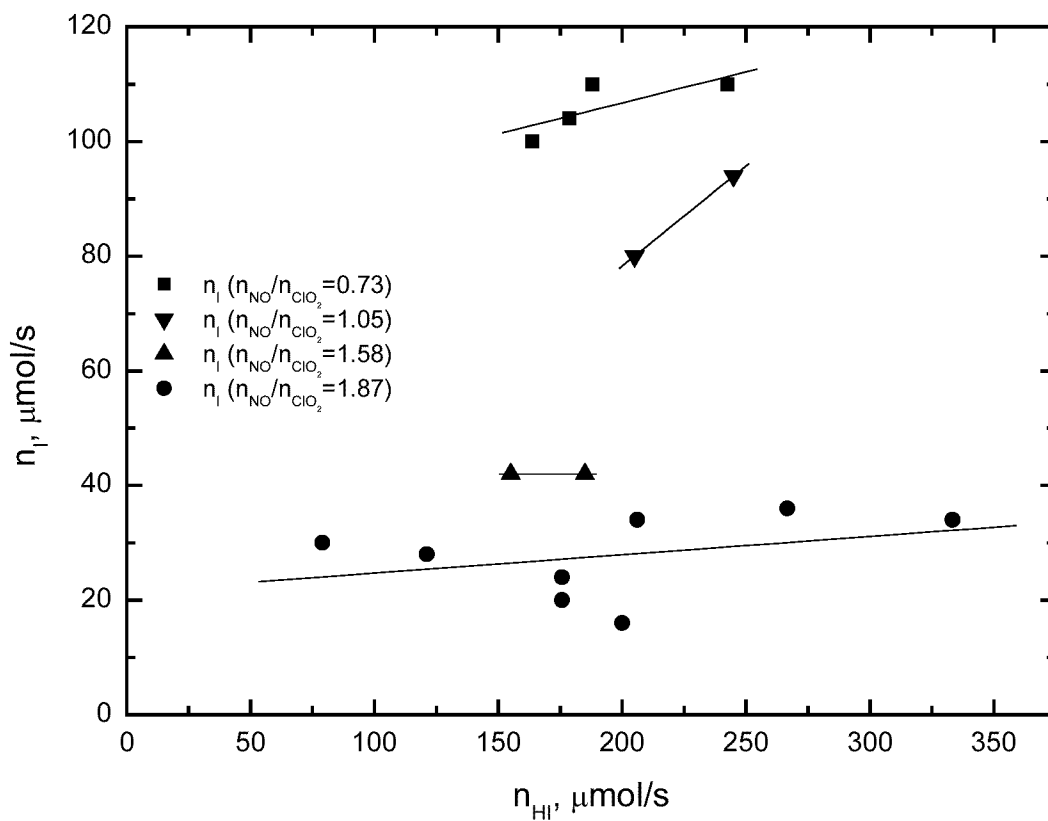


Fig.17. Atomic iodine flowrate as a function of the initial HI flowrate measured in the first optical cell for four different flowrates of NO:ClO₂ ratio, at 150 μmol NO(I)/s and 150 μmol NO(II)/s.

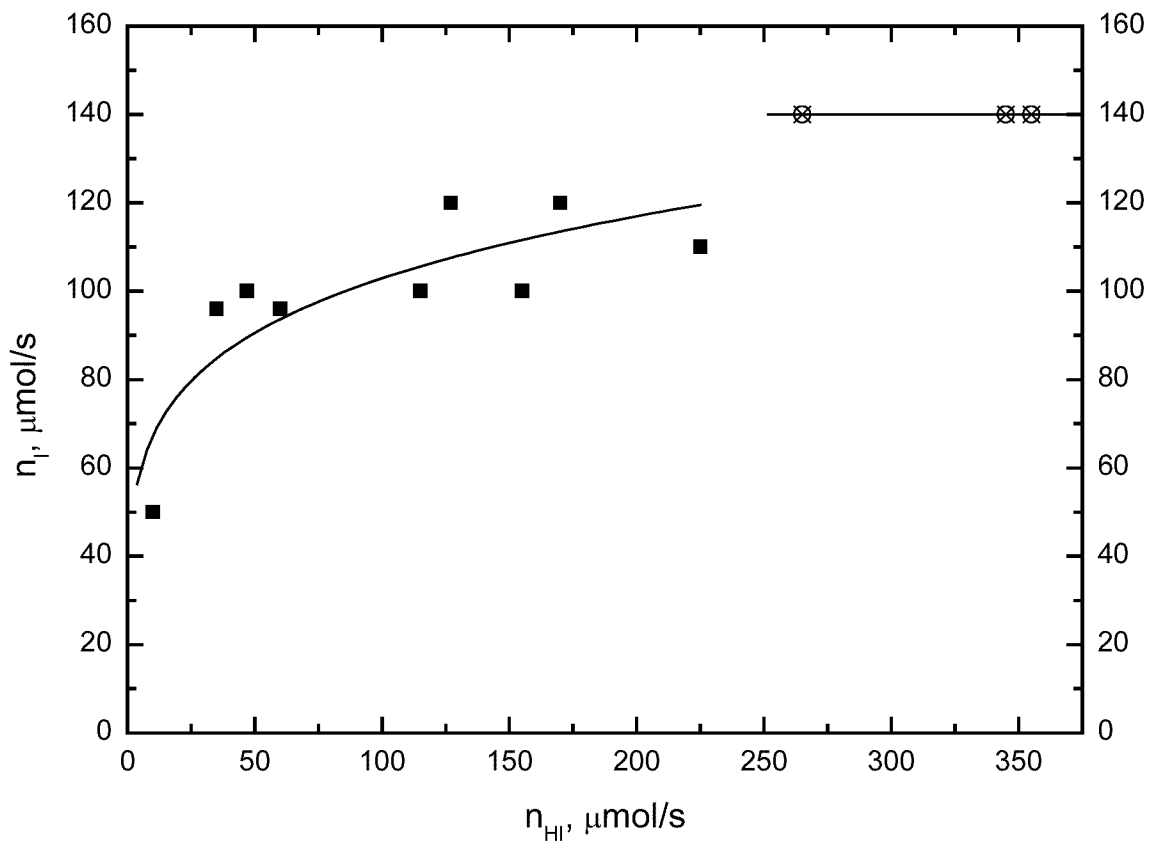


Fig.18. Atomic iodine flowrate as a function of the initial HI flowrate measured by the diode probe laser for two flowrates of ClO_2 . Initial flowrates: $125 \mu\text{mol ClO}_2/\text{s}$, $150 \mu\text{mol NO(I)}/\text{s}$, and $145 \mu\text{mol NO(II)}/\text{s}$ (squares); $190 \mu\text{mol ClO}_2/\text{s}$, $154 \mu\text{mol NO(I)}/\text{s}$, and $146 \mu\text{mol NO(II)}/\text{s}$ (circles).